Acta Pharmaceutica Sinica B 2023;13(8):3365−3381

Chinese Pharmaceutical Association
Institute of Materia Medica, Chinese Academy of Medical Sciences

Acta Pharmaceutica Sinica B

www.elsevier.com/locate/apsb
www.sciencedirect.com

ORIGINAL ARTICLE

Potentiation of PIEZO2 mechanically-activated currents in sensory neurons mediates vincristine-induced mechanical hypersensitivity

Mingli Duan[a,b,c,d,e,†], **Yurui Jia**[a,b,c,d,e,†], **Lifang Huo**[a,b,c,d,e,f,†], **Yiting Gao**[a,b,c,d,e], **Jia Wang**[a,b,c,d,e], **Wei Zhang**[f,b,c], **Zhanfeng Jia**[a,b,c,d,e,*]

[a]*Department of Pharmacology, Hebei Medical University, Shijiazhuang 050017, China*
[b]*Center of Innovative Drug Research and Evaluation, Institute of Medical Science and Health, Hebei Medical University, Shijiazhuang 050017, China*
[c]*The Key Laboratory of Neural and Vascular Biology, Ministry of Education, Shijiazhuang 050017, China*
[d]*The Key Laboratory of New Drug Pharmacology and Toxicology, Shijiazhuang 050017, China*
[e]*The Hebei Collaboration Innovation Center for Mechanism, Diagnosis and Treatment of Neurological and Psychiatric Disease, Shijiazhuang 050017, China*
[f]*Department of Pharmacology, Institute of Chinese Integrative Medicine, Hebei Medical University, Shijiazhuang 050017, China*

Received 9 December 2022; received in revised form 8 March 2023; accepted 14 March 2023

KEY WORDS

Vincristine;
Peripheral neuropathic pain;
Mechanical hypersensitivity;
Dorsal root ganglion neurons;
PIEZO2 mechanically-activated currents;

Abstract Vincristine, a widely used chemotherapeutic agent for treating different cancer, often induces severe peripheral neuropathic pain. A common symptom of vincristine-induced peripheral neuropathic pain is mechanical allodynia and hyperalgesia. However, mechanisms underlying vincristine-induced mechanical allodynia and hyperalgesia are not well understood. In the present study, we show with behavioral assessment in rats that vincristine induces mechanical allodynia and hyperalgesia in a PIEZO2 channel-dependent manner since gene knockdown or pharmacological inhibition of PIEZO2 channels alleviates vincristine-induced mechanical hypersensitivity. Electrophysiological results show that vincristine potentiates PIEZO2 rapidly adapting (RA) mechanically-activated (MA) currents in rat dorsal root ganglion (DRG) neurons. We have found that vincristine-induced potentiation of PIEZO2 MA currents is due to the enhancement of static plasma membrane tension (SPMT) of these cells following vincristine

*Corresponding author. Tel.: +86 311 86266343.
E-mail address: jiazf@hebmu.edu.cn (Zhanfeng Jia).
[†]These authors made equal contributions to this work.
Peer review under the responsibility of Chinese Pharmaceutical Association and Institute of Materia Medica, Chinese Academy of Medical Sciences.

https://doi.org/10.1016/j.apsb.2023.05.010

Whole-cell patch-clamp recording;
Membrane tension;
Microtubules

treatment. Reducing SPMT of DRG neurons by cytochalasin D (CD), a disruptor of the actin filament, abolishes vincristine-induced potentiation of PIEZO2 MA currents, and suppresses vincristine-induced mechanical hypersensitivity in rats. Collectively, enhancing SPMT and subsequently potentiating PIEZO2 MA currents in primary afferent neurons may be an underlying mechanism responsible for vincristine-induced mechanical allodynia and hyperalgesia in rats. Targeting to inhibit PIEZO2 channels may be an effective analgesic method to attenuate vincristine-induced mechanical hypersensitivity.

1. Introduction

Vincristine (VCR), a potent cytostatic alkaloid that prevents tubulin polymerization from soluble dimers into microtubules, is widely used as a chemotherapeutic agent to treat a variety of cancer[1−5]. Peripheral neuropathic pain is commonly induced by VCR in chemotherapy and it is a major adverse effect that limits the effective doses of VCR for cancer treatment[1,5−7]. Recently, VCR liposomes, a new kind of carrier-based smart drug delivery form, is developed for enhancing therapeutic effects with minimized systemic adverse effects of VCR[8]. VCR-induced neuropathic pain is commonly manifested with mechanical hypersensitivity, paresthesias and numbness in a stocking-and-glove distribution fashion in humans[9−11]. In experimental mammals, systemic administration of lower dose of VCR (< 100 μg/kg/day) induced mechanical allodynia and hyperalgesia without motor dysfunctions, and thermal hypersensitivity was not observed[9,10,12,13]. However, the mechanisms underlying VCR-induced mechanical hypersensitivity remain to be unclear. Clinically, mechanical allodynia is defined as pain induced by innocuous mechanical stimuli such as brushing and gentle touch; mechanical hyperalgesia is defined as exaggerated pain sensations induced by mild noxious mechanical stimuli such as pinch and pressure. These abnormal sensory responses occur under a number of pathological conditions including patients receiving chemotherapy such as VCR treatment[14,15].

A key step of sensing mechanical stimuli is mechanotransduction, a process by which mechanical energy is transduced into electrical signals at the peripheral endings of primary afferent nerves whose cell bodies are resided in DRGs and trigeminal ganglions. PIEZO channels, including PIEZO1 and PIEZO2, have been identified as *bona fide* mammalian mechanotransducers by producing mechanically-activated (MA) currents under sensing mechanical stimuli[16−18]. Based on their inactivation kinetics (also known as decay time constant, τ), the MA currents were classified into three types, rapidly adapting (RA, $\tau < 10$ ms), intermediately adapting (10 ms $< \tau <$ 30 ms) and slowly adapting ($\tau > 30$ ms)[19−21]. PIEZO2 channels are shown to mediate sufficiently the RA MA currents in DRG neurons and cutaneous Merkel cells and are required for sensing gentle touches[16,22−24]. For the discovery that PIEZO channels, especially PIEZO2 channels, are “the receptors of touch”, Dr. Ardem Patapoutian was awarded the Nobel Prize in Physiology or Medicine in 2021 (https://www.nobelprize.org/prizes/medicine/2021/summary/). PIEZO2 channels are extensively expressed in almost all DRG neurons in rodent animals[25,26]. Studies with either DRG neuron-specific PIEZO2 knockout mice or human patients with loss of function mutations in PIEZO2 gene have demonstrated that loss of PIEZO2 expression and function leads to the impairment of sensory responses to gentle touch and suppression of mechanical allodynia[22,25,27−29].

Given that PIEZO2 channels play important roles in mechanotransduction in primary afferent nerves, we hypothesize that PIEZO2 may be involved in mechanical hypersensitivity in VCR-induced peripheral neuropathy.

2. Materials and methods

2.1. Chemicals and antibodies

All chemicals were purchased from Sigma (Sigma−Aldrich LLC, St. Louis, MO, USA). Antibodies specific to PIEZO2 (NBP1-78624) were purchased from Novus Biologicals (Novus Biologicals LLC, Littleton, CO, USA). Antibodies specific to β-actin and secondary antibodies were purchased from Abcam (Abcam, Cambridge, UK).

2.2. Animals

Male Sprague−Dawley (SD) rats (6 to 8-weeks-old; 110−130 g) were used. Animal care and use conformed to the guidelines of the local Animal Care and Use Committee at Hebei Medical University (Shijiazhuang, China).

2.3. Animal model of mechanical hypersensitivity

VCR (0.05 mg/kg/day, diluted to 0.15 mL in saline, Tocris) was administered with an intraperitoneal injection (i.p.) using a 5-days-on, 2-days-off schedule as previously described[12]. This VCR treatment regimen produced hypersensitivity to mechanical stimuli in animals following 3−5 days of treatment. To verify the current dose of VCR did not affect motor functions and thermal sensations of animals, Rota-rod test, hot (52 °C) and cold (4 °C) plate test and Hargreaves test were performed and results were shown (Supporting Information Fig. S1).

2.4. Focal application to knock down PIEZO2 by shRNA interference in DRG in vivo

PIEZO2-shRNA lentiviral particles were focally applied to knock down the expression of PIEZO2 in DRG neurons *in vivo*. PIEZO2-(sc-270372-V)[23] and scrambled shRNA lentiviral particles were purchased from Santa Cruz Biotech (CA, USA). PIEZO2- or scrambled shRNA lentiviral particles were injected into DRGs. Five days later, VCR was injected (i.p.) to rats to induce

mechanical hypersensitivity. After behavioral assessment, the injected DRGs were harvested and PIEZO2 expression was examined in DRG neurons by immunostaining.

Animal surgery and focal application of shRNA lentiviral particles were performed as previously described[30]. In brief, male SD rats were anesthetized with injection (i.p.) of sodium pentobarbital (60−80 mg/kg). A midline incision was made at the L4−L6 spinal level of rats, and the L5 was identified at the midpoint of a link between both sides of the iliac crest. A 0.8-mm hole (∼1 mm off the inferior edge of the transverse process) was drilled through the transverse process over the L4 and L5 DRG. Approaching of a ganglion was verified by the twitch of the paw. The microinjector (Hamilton Co.) contained 3 μL solution of shRNA lentiviral particles was inserted into DRG to a depth of 500 μm through the hole. The shRNA lentiviral particles were injected slowly into each L4 and L5 DRG on one side, and the needle was removed 5 min after the injection was completed. The incision was closed with sutures. Intramuscular injection of benzylpenicillin (19 mg/0.1 mL) was given immediately after surgery. Postoperatively, rats were housed individually in plastic cages with sawdust flooring and supplied with water and food ad libitum. Animals were left to recover for at least 3 days before receiving VCR injection (i.p.) to induce mechanical neuropathy model.

2.5. *Animal behavioral measurement*

2.5.1. *von Frey test*

In each test, a rat was placed in a transparent plastic chamber (length × width × height = 20 cm × 10 cm × 14 cm) suspended above a wire mesh platform (Ugo Basile, Italy). After habituation for 15 min, the mechanical sensitivity of rat's right hind paws was examined using von Frey filaments (Ugo Basil, Italy). A series of von Frey filaments (force range from 0.16 to 26 g) were used sequentially in ascending order to push against the plantar surface of the hind paws. Each filament was applied to the plantar surface five times with a 10-s inter-trial interval. For each trial, the filament was applied until buckling of the filament occurred and was then held for 5 s. The withdrawal threshold was defined as the force value of a filament that produced 3 hind paw withdrawals in response to five stimuli. In each experiment, the baseline withdrawal threshold was first measured 15 min before the injection of testing compounds. The intraplantar hind paw of the rat was injected with one of the following solutions in a volume of 100 μL: saline solution (as Vehicle1); 0.5% dimethylsulfoxide (DMSO) saline solution (as Vehicle2); CD (1 mmol/L) in 0.5% DMSO saline solution; Gd^{3+} (0.3 mmol/L) in saline solution. Withdrawal thresholds were then measured at 15, 30, 60, and 90 min after the injection. To test for a less acutely developing allodynia effect of VCR, the withdrawal threshold was measured each day (Monday through Friday) before that day's injection of VCR.

2.5.2. *Randall−Selitto test*

Nociceptive withdrawal thresholds were examined and quantified by Randall−Selitto (Ugo Basile, Italy) mode pressure test. The Randall−Selitto device applies a linearly increasing mechanical force to the dorsum of the rat's hind paw through the cone head of a cone, while the plantar surface of the hind paw was against the top of a cylinder. In order to make sure that the mechanical force was applied on the plantar surface of the hind paw, we modified the direction of the mechanical stimulus device. The cone head and cylinder were exchanged so that the plantar surface of the hind paw was against the cone head while the dorsum of the hind paw received the mechanical force through the bottom of a cylinder. In each test, rats were habituated for 10 min to the testing procedure. The baseline nociceptive withdrawal threshold was first measured 15 min before the injection of testing compounds. The intraplantar hind paw of the rat was then injected with one of the following solutions in a volume of 100 μL: saline solution; 0.5% DMSO saline solution; CD (1 mmol/L) in 0.5% DMSO saline solution; Gd^{3+} (0.3 mmol/L) in saline solution. Nociceptive withdrawal thresholds were then measured at 15, 30, 60, and 90 min after the injection. To test for a less acutely developing hyperalgesic effect of VCR, the nociceptive withdrawal threshold was measured each day (Monday through Friday) before that day's injection of VCR.

2.5.3. *Rota-rod test*

Rota-rod test was performed as previously described[31] to assess motor coordination in rats. Briefly, rats were trained to remain on a treadmill device (Jixing Rota-Rod, Hebei, China) with slowly revolving rods of 6 cm diameter at 30 rpm for 60 s. Rats that were able to remain on the rod for 180 s or longer were selected and randomly divided into control group (Veh) and VCR group (VCR) of 8 rats per group. After VCR treatment, rats were placed individually on the revolving rod at intervals of 30 min, up to 60 min. If an animal failed more than once to remain on the rod for 3 min, the test was considered positive, meaning there was a lack of motor coordination.

2.5.4. *Hot or cold plate test*

In the hot plate test, control group (Veh) and VCR group (VCR) rats were placed on a hot plate at a certain temperature of 52 °C. Before (Day 0) and after (Days 2, 4, 6, 8, 10, and 12) the treatment, the response latency was recorded when the rats licking the hind paw or jumping. The cut-off time was 30 s to prevent scalding. In the cold plate test, control group (Veh) and VCR group (VCR) rats were placed on a cold plate at a certain temperature of 4 °C. Before (Day 0) and after (Days 2, 4, 6, 8, 10, and 12) the treatment, the response latency was recorded when the rats licking the hind paw or jumping. The cut-off time was 30 s to prevent frostbite.

2.5.5. *Hargreaves test*

Hargreaves test was performed by a radiant heat lamp source (PL-200, Taimeng Co., Chengdu, China). Briefly, the intensity of the radiant heat source was set at 25 ± 0.1%. Rats were individually placed into plexiglass cubicles placed on a transparent glass surface. The light beam from the radiant heat lamp located below the glass, was directed at the plantar surface of hindpaw. Time was recorded from the onset of radiant heat stimulation to the withdrawal of the hindpaw. The cut-off time was 30 s to prevent scalding. Three trials with an interval of 10 min were made for each rat, and scores from the three trials were averaged.

2.6. *Cell culture and transfection*

Primary cultures of DRG neurons were prepared from 6 to 8-weeks-old male SD rats using a previously described procedure[32]. Briefly, rats were anesthetized with isoflurane and sacrificed by decapitation. DRGs were rapidly dissected out bilaterally and incubated with 0.2% collagenase and 0.5% dispase for 1 h at 37 °C in a minimum essential medium for

suspension culture (Invitrogen). After digestion and trituration to dissociate neurons, DRG neurons were plated on glass coverslips pre-coated with poly-D lysine (12.5 μg/mL) and laminin (20 μg/mL in Hanks' buffered salt solution, BD Biosciences). The cells were cultured in minimum essential medium (Invitrogen) that contained 2.5S nerve growth factor (10 ng/mL; Roche Applied Science), 5% heat-inactivated horse serum (JRH Biosciences, Lenexa, KS), uridine/5-fluoro-2′-deoxyuridine (10 μmol/L), 8 mg/mL glucose, and 1% vitamin solution (Invitrogen). The cultures were maintained in an incubator at 37 °C with a humidified atmosphere of 95% air + 5% CO_2. Cells were used for patch clamp recordings after culturing for 2−5 days. In the knockdown experiment, DRG neurons were acutely cultured for 12 h and then incubated with scrambled shRNA or PIEZO2 shRNA for 24 h. Next, whole-cell patch clamp recordings were performed on these cells after recovery for 48 h. DRG neurons from VCR-induced neuropathic pain rats were cultured using the same protocol as described above. And then patch clamp recordings were performed on these cells within 24 h.

Human embryonic kidney (HEK293T cells) were plated onto 13 mm glass coverslips pre-coated with poly-D-lysine (100 μg/mL). Transfections were performed with X-tremeGENE HP DNA transfection reagent (Roche) according to the manufacturer's protocol. In addition, EGFP was co-transfected to identify the transfected cells. The PIEZO2 plasmid was purchased from Addgene (plasmid #81073).

2.7. *Electrophysiological recordings*

Electrophysiological recordings were performed as described in previous study[32]. Whole-cell patch-clamp recordings were applied to record MA currents in rat DRG neurons and PIEZO2 currents in PIEZO2 plasmid transfected HEK 293T cells at room temperature of 22−24 °C. Coverslips with cultured neurons were placed in a 0.5 mL recording chamber. The recording chamber was mounted on a stage of an Olympus IX71 inverted microscope (Olympus Corporation, Tokyo, Japan) and cells were continuously perfused at 2 mL/min with bath solution. The bath solution contained 145 mmol/L NaCl, 5 mmol/L KCl, 2 mmol/L $MgCl_2$, 2 mmol/L $CaCl_2$, 10 mmol/L glucose, 10 mmol/L HEPES, with an osmolarity of 320 mOsm and pH 7.35. The recording electrode internal solution contained 70 mmol/L Cs_2SO_4, 5 mmol/L KCl, 2.4 mmol/L $MgCl_2$, 0.5 mmol/L $CaCl_2$, 5 mmol/L EGTA, 10 mmol/L HEPES, 5.0 mmol/L Na_2ATP, 0.33 mmol/L GTP-Tris salt, with pH 7.35 and osmolarity of 320 mOsm. The recording electrodes were fabricated from thin wall borosilicate glass capillaries using a Flaming P-97 puller (Sutter Instrument Co., Novato, CA, USA) and had resistances of 3−5 MΩ. Junction potential between bath and electrode solution was calculated to be 11 mV and was corrected for the data analysis. Voltage clamp recordings were performed with cells held at −71 mV (command voltage of −60 mV minus 11 mV for junction potential correction). Signals were recorded with an Axonpatch 200B amplifier, filtered at 2 kHz, and sampled at 5 kHz using pCLAMP 10.7 (Axon Instruments; Molecular Devices, LLC, Sunnyvale, CA, USA). The protocol used to study PIEZO2 MA currents in DRG neurons was as follows: the cells were held at −71 mV and cell membranes were displaced by a heat-polished glass probe. The probe, with a ∼4 μm diameter tip, was positioned at an angle of 45° to the surface of the dish and its movement was controlled by a piezo-electric device (Physik Instruments, Auburn, MA, USA). The probe was moved at a speed of 0.5 μm/ms. Membrane displacements by the probe were visualized as live images, which were continuously captured by a CCD camera through a 40 × objective and displayed on an 11-inch monitor throughout each experiment. For most recordings, a fixed membrane displacement (6 or 7 μm, 500-ms duration) was applied immediately after breaking into the whole-cell mode and then continually applied at an interval of 2 min for up to 30 min. In some experiments, a series of mechanical stimuli in 1-μm increments with 500-ms duration of each step was applied to elicit MA currents. The interval was 6 s when the displacement steps were applied. Because membrane displacement might affect membrane seal to change access resistance, membrane properties were continually monitored during each recording. This was achieved by applying 5-mV test pulses. Data were discarded if membrane access resistance changed during recordings. For intracellular hypertonicity, hypertonic recording pipette solution was used, and the solution was similar to normal pipette solution except the osmolarity was adjusted with sucrose to 420 mOsm. In experiments to introduce hypertonicity extracellularly, a hypertonic bath solution was used, and the solution was similar to normal bath solution except the osmolarity was adjusted with sucrose to 420 mOsm. Cell diameters were measured from images captured by a digital camera, and a cell diameter was calculated as the average of the longest and shortest widths of the cell.

Whole-cell patch clamp recording data were analyzed using Clampfit 10.7 software. The threshold for eliciting PIEZO2 MA currents was defined as the minimum membrane displacement that evoked a visible inward MA current. The onset latency of a PIEZO2 MA current in response to a membrane displacement was the time delay from the contact of cell membranes by stimulation probe to the initiation of the PIEZO2 MA current. Decay time constant of a PIEZO2 MA current was obtained by fitting the current decay phase in the range of 10%−90% with a single exponential equation.

2.8. *Membrane tension measurement*

The SPMT of cultured rat DRG neurons was measured using the micropipette aspiration technique as previous study described[32]. Briefly, micropipette was pulled from thin wall borosilicate glass capillaries using Flaming P-97 puller. The tips of the micropipettes had internal diameters ranged between 5 and 8 μm depending on cell sizes, and the tip of each micropipette was in a cylindrical shape at a length of approximately 10 μm. Micropipettes were filled with bath solution that contained 5% horse serum to allow the cell membrane to move smoothly into the micropipette during aspiration. The micropipette was affixed on a head stage of a high-speed pressure clamp (HSPC) device, and the head stage was mounted on a holder of a micromanipulator to allow fine control of the position of the micropipette. At the beginning of each experiment, the pressure in the pipette was equilibrated to the atmospheric pressure. The micropipette was moved horizontally toward a cell until its tip was in full contact with the cell membrane. To apply aspiration, steps of negative pressures were generated by HSPC device, and the negative pressures were delivered to the micropipette tip *via* the head stage of the HSPC. The HSPC was controlled, and pressure steps were programmed using pCLAMP 10.7 (Axon Instruments). Each negative pressure step was at 0.01 mmHg and was applied until membrane projection was stabilized at a certain length before advancing to the next pressure step. A test for a single pressure

step usually took ~2 min. The negative pressure steps were continually applied to the cell until obtaining the negative pressure at which the membrane projection reached the length of the radius of the micropipette tip. During each negative pressure step, real-time images of membrane deformation were acquired by a CCD camera and displayed on a 17-inch video monitor to track the membrane projection that was aspirated into the pipette. Membrane tension was determined based on the law of LaPlace and Young-LaPlace Eq. (1) [33]

$$P_p = 2T_c \cdot \left(1 / R_p - 1 / R_c\right) \quad (1)$$

where T_c is the plasma membrane tension; R_c is the radius of the cell outside the pipette; R_p is the radius of the pipette; P_p is the pipette pressure to result in $L_p = R_p$; L_p is the length of membrane projection in the pipette, and $P_p = P_c$ (intracellular pressure) when $L_p = R_p$. The value of SPMT at each time point represents averaged SPMT around that time point with the time bin of ±1 min.

2.9. Immunostaining

SD rats were transcardially perfused with 4% paraformaldehyde under terminal anesthesia (Sodium Pentobarbital, 80 mg/kg). Lumbar DRGs were removed and stored in 0.1 mol/L Phosphate Buffer (Sigma−Aldrich) followed by embedding in OCT (SAKURA), then postfixed in 4% paraformaldehyde for 1 h prior to sectioning. DRG sections were cut at 35 μm using a vibrating microtome (Leica). Sections were washed once with 0.1 mol/L phosphate buffer saline (PBS) (Sigma−Aldrich), incubated for 30 min in 37 °C with 0.3% Triton X-100/PBS buffer and blocked for 2 h with blocking buffer (3% donkey serum in 0.1 mol/L PBS; Sigma−Aldrich). Sections were then incubated with primary anti-PIEZO2 antibody (1:200; Novus Biologicals, Littleton, CO, USA) overnight at 4 °C. Following 3 rinses with 1% goat serum PBS solution, sections were further incubated with the secondary antibody conjugated to Alexa Fluor 594 (1:500; Invitrogen, Carlsbad, CA, USA) for 4 h at room temperature. Sections were washed with PBS 3 times and placed on microscope slides. Staining was visualized using a confocal fluorescent microscope (Leica SP5, Leica).

For the immunostaining of individual DRG neurons, planted cells were incubated at room temperature for 15 min in 4% paraformaldehyde solution and further incubated for 2 h in a mixture solution of 0.3% TritonX-100 and 4% paraformaldehyde. After three rinses with PBS, the cells were incubated for 2 h at room temperature with a 2% Triton X-100 solution. The cells were rinsed two times with 1% goat serum PBS and then incubated for 1 h in a solution of 4.5% normal goat serum in PBS with 0.3% Triton X-100 to block nonspecific antibody binding. The cells were incubated with a primary anti-PIEZO2 antibody overnight at 4 °C. Following three rinses with 1% goat serum PBS solution, the cells were further incubated with a secondary antibody for 1 h at room temperature. The secondary antibody (1:200 in 1% goat serum PBS solution) was a goat anti-rabbit IgG conjugated with Alexa-488 (Jackson Immuno Research). The cells were rinsed three times with 1% goat serum PBS solution, and coverslipped with a glycerol-based anti-photobleach medium. Cell images were taken under a confocal fluorescent microscope. The values of immunofluorescence (IF) intensity were measured along the line over cells.

2.10. Reverse transcription-quantitative polymerase chain reaction (RT-qPCR)

Total RNA from rat DRGs was extracted using a commercial RNA isolation kit (RNAiso, Takara Bio, Inc., Otsu, Japan). Isolated RNA was dissolved in 20 μL diethyl pyrocarbonate-treated (DEPC-treated) water and reverse-transcribed using an RT reagent kit (PrimeScript with gDNA Eraser, Takara Bio, Inc.) and a thermal cycler (Bio-RAD, CA, USA). Quantitative PCR reaction was performed using a kit (SYBR Premix Ex TaqII [Tli RNase H Plus], Takara Bio, Inc.), and the fluorescent DNA was detected and quantified with an Eco System (Gene Company Limited, HK, China). The PCR primer sequences were as follows: PIEZO2 forward: TAAGGAGTTCATCGGCAATA, and reverse: AGGCAGCCAAACAGCAAT; *GAPDH* forward: GGAGATTACTG CCCTGGCTCCTAGC, and reverse: GGCCGGACTCTTCG-TACTCCTGCTT. *GAPDH* was used as an internal control. Each test was performed in triplicate. Gene expression was calculated from the cycle threshold (Ct) value, and the $2^{-\Delta\Delta Ct}$ method was used.

2.11. Western blot analysis

Proteins were extracted from DRGs, separated by electrophoresis on a 10% SDS-polyacrylamide gel, and transferred onto PVDF membranes. Nonspecific binding sites were blocked with 5% skim milk in Tris-buffered saline solution with Tween-20 for 2 h at room temperature. Membranes were then incubated with primary antibodies overnight at 4 °C. β-Actin was used as a housekeeping protein. The second day, the blots were incubated with secondary antibodies for 2 h at room temperature and visualized by the Odyssey Fc System (LI-COR, NE, USA). Densitometry of the protein bands was performed using ImageJ 1.50i software (National Institutes of Health). The experiments were repeated at least three times.

2.12. Statistical analysis

Data are presented as the mean ± standard error of the mean (SEM) for the indicated number of independently conducted experiments, and analyzed with SPSS (SPSS, Inc., Chicago, IL, USA). The concentration−effect curve for VCR-induced potentiation of PIEZO2 MA currents was fitted by Hill function. Statistical significance was evaluated by either a Student's *t*-test or a one-way analysis of variance followed by multiple comparison using Student's *t*-test without corrections[32,34]. χ^2 test was used to analyze the difference in the amounts of PIEZO2-positive neurons between control rats and VCR-pain model rats. $P < 0.05$ was considered to indicate a statistically significant difference.

3. Results

3.1. Knockdown of PIEZO2 expression in DRG neurons prevents VCR-induced mechanical hypersensitivity

To determine the essential role of PIEZO2 in mediating VCR-induced mechanical hypersensitivity, we knocked down the expression of PIEZO2 in rat DRG neurons using shRNA interference. Solution of *PIEZO2* shRNA or scrambled shRNA lentiviral particles was directly administrated in L4 and L5 DRG

tissues through microinjection under animal surgery. A group of rats received microinjection of vehicle was used as blank control. After surgery, rats recovered for 3 days before receiving i.p. injection of VCR. A subgroup of *PIEZO2* shRNA-treated rats received i.p. injection of vehicle (*PIEZO2* shRNA + *Veh2*) was used as the control for VCR treatment rats (*PIEZO2* shRNA + *VCR*). We then performed the behavioral test *in vivo*. Mechanical allodynia and hyperalgesia were identified by the reduction of hind paw withdrawal threshold and nociceptive withdrawal threshold which were measured by von Frey filament (Fig. 1A) and Randall−Selitto pressure test (Fig. 1B), respectively. Basic thresholds were measured before shRNA lentiviral particles administration. One day before i.p. injection of VCR, the thresholds were also measured. As shown in Fig. 1A and B, there was no significant difference in basic withdrawal threshold and nociceptive withdrawal threshold among the four groups (Fig. 1A and B). At the 6th day of VCR administration, the withdrawal thresholds of scrambled shRNA group rats were significantly reduced compared with that of vehicle-treated rats (Fig. 1A). Additionally, scrambled shRNA group rats showed persistent lower withdrawal thresholds following VCR administration (Fig. 1A). At the 4th day of VCR administration, the withdrawal thresholds of *PIEZO2* shRNA group rats were significantly increased compared with that of scrambled shRNA group rats (Fig. 1A). After that, rats in *PIEZO2* shRNA + *VCR* group displayed gradually elevated withdrawal thresholds, which were even much higher than that of vehicle-treated rats (Fig. 1A). While the withdrawal thresholds of *PIEZO2* shRNA + *Veh2* group rats significantly increased at the 4th day and gradually elevated along the experimental schedule. Compared to *PIEZO2* shRNA + *Veh2* group rats, the withdrawal thresholds of *PIEZO2* shRNA + *VCR* group rats significantly reduced in the later schedule (Fig. 1A). At the 3rd day of VCR administration, the nociceptive withdrawal thresholds of scrambled shRNA group rats were significantly reduced compared with that of vehicle-treated rats (Fig. 1B). Then, scrambled shRNA group rats showed sustained lower nociceptive withdrawal thresholds following VCR administration (Fig. 1B). *PIEZO2* shRNA interference (*PIEZO2* shRNA + *VCR*) restored the nociceptive withdrawal thresholds to the levels of vehicle treated rats (Fig. 1B). As a control, the nociceptive withdrawal thresholds of *PIEZO2* shRNA + *Veh2* group rats showed a small but significant reduction in the later schedule (Fig. 1B). Notice that an interesting phenomenon was *PIEZO2* shRNA + *VCR* group rats showed significant increase of the thresholds in von Frey test while showed no significant changes in Randall−Selitto test when compared to the normal level (Fig. 1A and B).

These different changes may be due to the role of PIEZO2 not only in mediating light touch sensation (von Frey model)[22,23,25], but also in suppressing mechanical pain (Randall−Selitto model)[24]. Knockdown of PIEZO2 certainly inhibited its role, as the touch receptor, resulting in touch retardation which even belied the effect of VCR (Fig. 1A). While knockdown of PIEZO2 also relieved its role in suppression of mechanical pain so that the nociceptive threshold should not be increased or be even decreased (Fig. 1B). To confirm PIEZO2 was knocked down in DRG neurons, immunostaining experiments were performed to determine PIEZO2 immunoreactivity in *PIEZO2* shRNA and scrambled shRNA groups. As shown in Fig. 1C and D, *PIEZO2*-shRNA knockdown significantly reduced the PIEZO2-immunoreactivity in DRG neurons in comparison with the control group (Fig. 1C and D). The IF intensity of PIEZO2 was 168.9 ± 5.3 in scrambled shRNA group and significantly reduced to 96.9 ± 3.6 ($P < 0.001$) in *PIEZO2*-shRNA group (Fig. 1D). Taken together, these results indicate that knockdown of PIEZO2 in rat DRG neurons prevents VCR-induced mechanical allodynia and hyperalgesia.

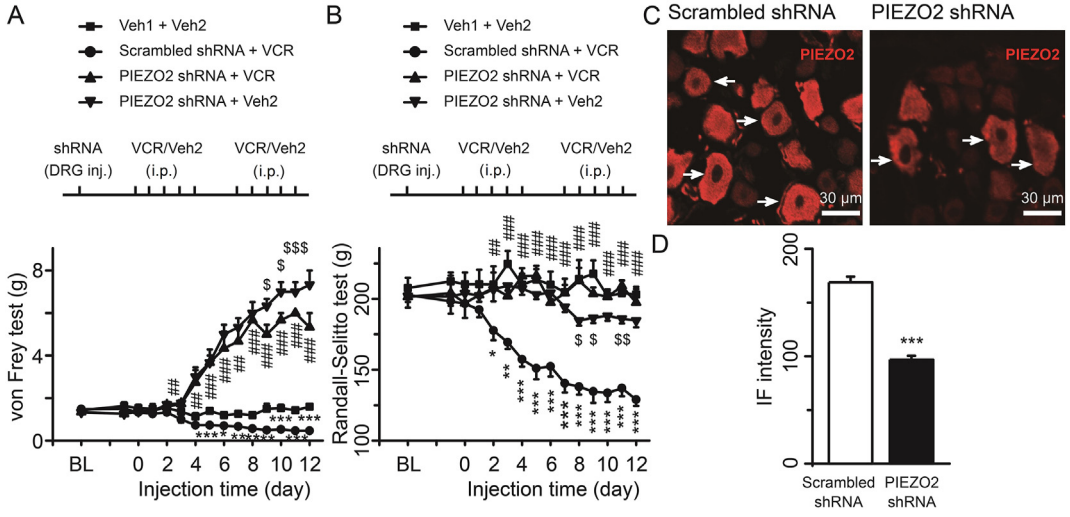

Figure 1 Focal knockdown of PIEZO2 MA channel in DRG suppressed VCR-induced mechanical hypersensitivity. Mechanical allodynia (A) and mechanical hyperalgesia (B) were determined by the reduction of withdrawal thresholds measured with von Frey filaments and nociceptive withdrawal thresholds measured with Randall−Selitto set, respectively. ShRNA (DRG inj.) and VCR (i.p., 50 μg/kg/day) administration were performed following the schedule (above). Each group represented by different symbols is shown in top place. $n = 8$ each group. (C) Immunostaining of PIEZO2 in DRG neurons in scrambled shRNA + *VCR* (left) and *PIEZO2* shRNA + *VCR* group (right), respectively. (D) IF intensity of PIEZO2 in scrambled shRNA + *VCR* (open bar) and *PIEZO2* shRNA + *VCR* group (solid bar). $n = 83$ and 81 in Cont and VCR group, respectively. Data are shown in mean ± SEM; $^{*/\$}P < 0.05$, $^{**/\#\#/\$\$}P < 0.01$, $^{***/\#\#\#/\$\$\$}P < 0.001$.

3.2. *Pharmacological inhibition of PIEZO2 channel activity eliminates VCR-induced mechanical hypersensitivity*

To further determine the role of PIEZO2 MA channels in VCR-induced mechanical allodynia and hyperalgesia, we examined behavioral outcomes in rats following the inhibition of PIEZO2 MA channels with pharmacological agents. In this set of experiments, basic thresholds were measured before and after i.p. injections of VCR (Fig. 2A and D). Four days after VCR treatment, rats showed a significant reduction in mechanical withdrawal threshold and nociceptive withdrawal threshold (Fig. 2A and D). On Day 9 following VCR application, gadolinium (Gd^{3+}, 0.3 mmol/L), a blocker of PIEZO2 MA channel[15] was subcutaneously injected into the hind paw and the withdrawal thresholds were measured. We found that Gd^{3+} significantly increased the mechanical withdrawal threshold and nociceptive withdrawal threshold of VCR-neuropathic pain rats (Fig. 2B and E). On Day 11 following VCR administration, we measured the mechanical withdrawal threshold and nociceptive withdrawal threshold following subcutaneous injection of CD, a disruptor of actin filaments. We have previously shown that CD inhibited PIEZO2 MA currents in rat DRG neurons by reducing the SPMT of DRG neurons[32]. In the present study, we found that CD also significantly increased the mechanical withdrawal threshold and nociceptive withdrawal threshold of VCR-neuropathic pain rats (Fig. 2C and F). These results further support that PIEZO2 MA channels may be involved in VCR-induced mechanical hypersensitivity.

3.3. *The expression of PIEZO2 is not changed in individual DRG neurons in VCR-induced mechanical hypersensitivity rats*

To address whether the PIEZO2-dependent mechanical allodynia and hyperalgesia induced by VCR are due to the elevated expression of PIEZO2 channels, we measured the PIEZO2 expression at mRNA level and protein level in DRG, respectively. Surprisingly, we found that the expression of PIEZO2 was significantly downregulated in DRGs in VCR-neuropathic pain rats either at mRNA level or at protein level compared with that of control group rats (Fig. 3A–C). The mRNA expression of *PIEZO2* was reduced by 59% in VCR-neuropathic pain group rats ($P < 0.001$) compared with that of the control group rats (Fig. 3A). Consistently, the protein expression of PIEZO2 in VCR-neuropathic pain rats was also significantly reduced by approximately 18% ($P < 0.05$) compared with that of control rats (Fig. 3B and C). In addition, the expression of β-tubulin was not significantly affected by VCR (Fig. 3B and C). These results indicate that the changes of PIEZO2 expression are not directly related to the disruption of microtubules with VCR treatment. Using immunostaining assay we further measured the expression

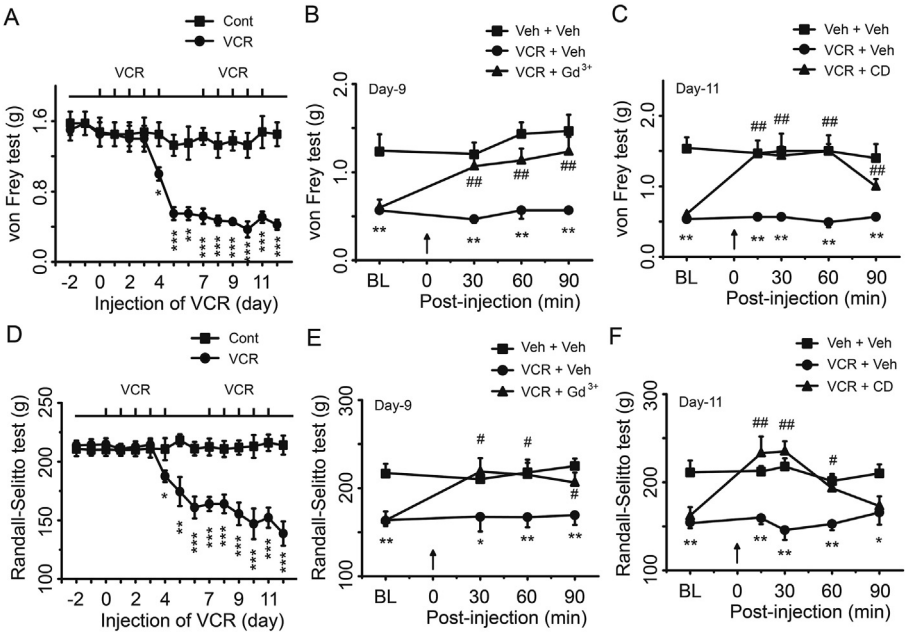

Figure 2 Pharmacological inhibition of PIEZO2 MA channel activity suppressed VCR-induced mechanical hypersensitivity. Mechanical allodynia (A) and mechanical hyperalgesia (D) were elicited by VCR administration (i.p., 50 μg/kg/day) following the schedule (above). At the 9th day of VCR administration, mechanical withdrawal thresholds (B) and nociceptive withdrawal thresholds (E) were tested before (baseline, BL) and at 30, 60 and 90 min after intraplantar injection (arrow at 0 min) of $GdCl_3$ (300 μmol/L, 100 μL) (triangle) or the same volume of vehicle (circle). A group of rats was considered as negative control (square). At the 11th day of VCR administration, mechanical withdrawal thresholds (C) and nociceptive withdrawal thresholds (F) were tested before (baseline, BL) and at 30, 60 and 90 min after intraplantar injection (arrow at 0 min) of CD (1 mmol/L, 100 μL) (triangle) or the same volume of vehicle (circle). A group of rats was considered as negative control (square). Data are shown in mean ± SEM, $n = 8$ each group; $^{*/\#}P < 0.05$, $^{**/\#\#}P < 0.01$, $^{***}P < 0.001$.

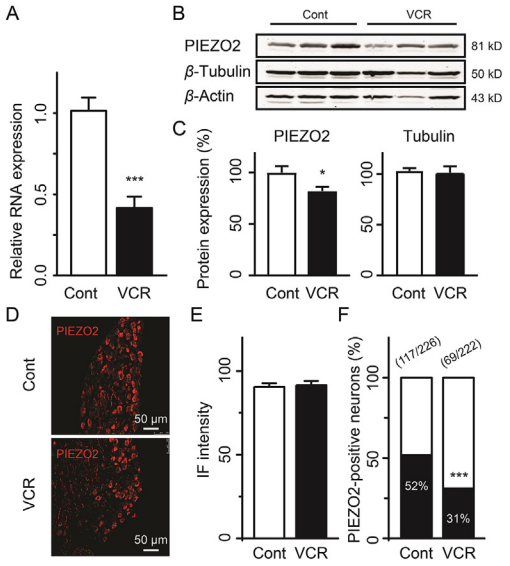

Figure 3 Expression of PIEZO2 in DRG neurons of VCR-induced neuropathic pain rats. (A) Relative mRNA expression of *Piezo2* in DRG of control rats (Cont) and VCR-induced pain model rats (VCR). Representative (B) and summary (C) data of PIEZO2 and Tubulin expression with Western blot assay in DRG of control rats (Cont) and VCR-pain model rats (VCR), respectively. β-Actin was used as control. $n = 12$ each group. Representative images (D) and IF intensity (E) of PIEZO2-positive DRG neurons of control rats (Cont) and VCR-pain model rats (VCR). $n = 254$ and 174 in Cont and VCR group, respectively. (F) The ratio of PIEZO2-positive DRG neurons to total DRG neurons in control rats (Cont) and VCR-pain model rats (VCR). The amounts of PIEZO2-positive DRG neurons and total DRG neurons of control rats (Cont) and VCR-pain model rats (VCR) are shown above the bars. Data are shown in mean ± SEM; $^{*}P < 0.05$, $^{***}P < 0.001$.

of PIEZO2 channels in DRG neurons. Interestingly, as shown in Fig. 3D and E, there was no significant difference in the IF intensities of PIEZO2 in individual DRG neurons between VCR-neuropathic pain rats and control rats (Fig. 3D and E). However, the ratio of PIEZO2-positive DRG neurons was significantly reduced from 52% (117 out of 226) of control rats to 31% (69 out of 222) of VCR-neuropathic pain rats (Fig. 3F, $P < 0.001$). These results indicate that the expression of PIEZO2 in individual DRG neurons was unchanged but the amounts of PIEZO2-positive neurons were significantly reduced in VCR-neuropathic pain rats. The remaining PIEZO2-positive DRG neurons might be sufficient to mediate VCR-induced mechanical hypersensitivity. However, here raised a question the unchanged expression of PIEZO2 in individual DRG neurons induced by VCR seemed in contrast to VCR-induced potentiation of PIEZO2 currents (below) and behavior observation obtained by PIEZO2 knockdown (Fig. 1A and B). One possibility is that VCR may induce PIEZO2 translocation (trafficking) from cytoplasm to the membrane in DRG neurons (see Discussion). Anyway, VCR-induced PIEZO2-dependent mechanical hypersensitivity in rats is not due to the upregulation of PIEZO2 expression in DRG neurons in rats.

3.4. *VCR potentiates PIEZO2 MA currents in rat DRG neurons*

We then examined the effects of VCR on PIEZO2 MA currents in DRG neurons using patch clamp technique. Before this experiment, we first examined the expression of PIEZO1 and PIEZO2 with Western blot assay in order to confirm that PIEZO2 was dominantly expressed in rat DRG neurons. Indeed, the bands of PIEZO2 were obvious while PIEZO1 was hard to be detected (Supporting Information Fig. S2). Next, PIEZO2 MA currents were elicited by a 7-μm membrane displacement on cultured rat DRG neurons with a mechanical stimulation probe. PIEZO2 MA currents were examined immediately after establishing the whole-cell patch-clamp (initial) and then continually tested every 2 min for up to 30 min. In this set of experiments, membrane tests were continually conducted to monitor the membrane resistance of the recorded cells, and cells whose membrane resistances were changed during recordings were discarded (Fig. 4A). VCR (5 μmol/L) was included in the recording pipette solution and applied intracellularly once whole-cell configuration was achieved. As shown in Fig. 4A and B, VCR treatment significantly potentiated PIEZO2 MA currents in rat DRG neurons. The amplitude of PIEZO2 MA currents was gradually increased following VCR application (Fig. 4A and B). For example, following VCR treatment the amplitudes of PIEZO2 MA currents increased to 2.4-fold ($n = 10$, $P < 0.05$) at 8 min, 3.2-fold ($n = 9$, $P < 0.001$) at 16 min, 6.6-fold ($n = 8$, $P < 0.001$) at 24 min and about 8.8-fold ($n = 8$, $P < 0.001$) at 30 min (Fig. 4A and B). We also examined the effect of VCR on PIEZO2 MA currents which were evoked at different membrane displacements. As shown in Fig. 4C–E, for membrane displacements from 1 to 7 μm in a 1-μm step increment, PIEZO2 MA currents elicited following VCR application were significantly larger than that of the control group. For example, at 7-μm membrane displacements, PIEZO2 MA currents were 725 ± 173 pA ($n = 10$, $P < 0.01$) and 190 ± 25 pA ($n = 10$) with and without the applications of 5 μmol/L VCR, respectively (Fig. 4D). In control group (Fig. 4C), PIEZO2 MA currents showed run-up phenomenon which was consistent with our previous observation[35]. In addition, the VCR-induced potentiation effect on PIEZO2 MA currents was concentration-dependently increased along the increasing VCR concentrations (0.2, 1, 5 and 25 μmol/L were tested respectively) (Fig. 4C and D). The concentration for 50% of maximal effect (EC_{50}) was 2.4 μmol/L (Fig. 4C and E). Knocking down the expression of PIEZO2 in DRG neurons using *PIEZO2* shRNA lentivirus, the VCR-induced potentiation of PIEZO2 MA currents was dramatically suppressed (Fig. 4F and G). For example, the PIEZO2 MA currents were reduced from 686 ± 142 pA ($n = 9$) in scrambled shRNA group to 82 ± 21 pA ($n = 10$, $P < 0.01$) in *PIEZO2* shRNA group under 7-μm membrane displacements (Fig. 4G). In summary, 45 DRG neurons were tested, 84.4% ($n = 38$) of them were potentiated by VCR, 15.6% ($n = 7$) showed no response (Supporting Information Fig. S3A–S3C). Among the 38 responsive cells, 13.2% of them ($n = 5$) were large cells (cell diameter >40 μm), 44.7% ($n = 17$) and 42.1% ($n = 16$) of them were medium (30–40 μm) and small cells (<30 μm), respectively (Supporting Information Fig. S3B). In addition, the potentiation effect of VCR on PIEZO2 currents was also verified in heterologous expression HEK 293T cells (Fig. 4H and I). As shown in Fig. 4I, VCR (5 μmol/L) intracellular treatment significantly increased PIEZO2 currents from 350 ± 163 pA ($n = 5$, Control) to 995 ± 160 pA ($P < 0.05$; $n = 4$, VCR) under 10-μm membrane displacements. Bath administration of D-

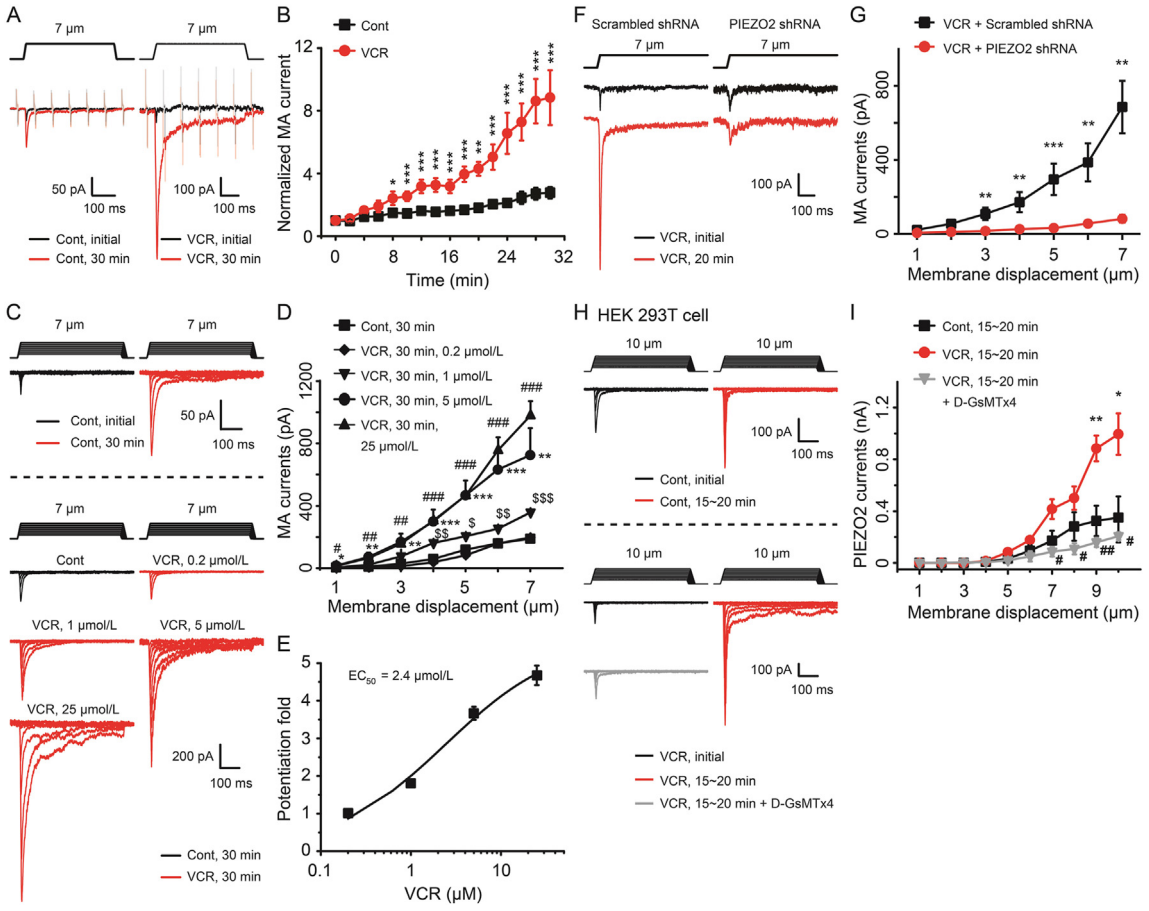

Figure 4 VCR potentiated PIEZO2 MA currents in rat DRG neurons and PIEZO2 transfected HEK 293T cells. (A) Sample traces showed the PIEZO2 MA currents evoked by a 7-μm membrane displacement (above) at the initial time (black) and 30 min (red) after establishing whole-cell mode patch recording with (right, VCR) or without (left, Cont) intracellular administration of VCR (5 μmol/L). The traces also included continual membrane tests by voltage steps of 5 mV at the interval of 100 ms (light color). (B) Summary data of the potentiation of PIEZO2 MA currents recorded with (red circle, VCR) or without (black square, Cont) intracellular application of VCR (5 μmol/L) over time. $n = 17$ and 10 in Cont and VCR group, respectively. (C) Representative traces of PIEZO2 MA currents elicited by a set of membrane displacements from 1 to 7 μm (above the current traces) in control group (Cont, above the dish line) and VCR intracellular treatment group at different concentrations (VCR, below the dish line). (D) Statistics for the potentiation of PIEZO2 MA currents treated intracellularly by different concentrations of VCR. The currents were evoked at 30 min and VCR was used at 0.2 μmol/L (black diamond, $n = 4$), 1 μmol/L (black inverted triangle, $n = 4$), 5 μmol/L (black circle, $n = 5$) and 25 μmol/L (black triangle, $n = 4$), respectively. $n = 7$ in Cont group. (E) Concentration−effect curve of VCR-induced potentiation of PIEZO2 MA currents in rat DRG neurons. The potentiation fold was evaluated from the effects induced by different concentrations of VCR at the 7-μm stimulation displacement. The EC_{50} is shown above. (F) Representative traces of PIEZO2 MA currents elicited by a 7-μm poking displacement (above) at the initial time (black trace) and 20 min (red trace) from 5 μmol/L VCR intracellularly treated DRG neurons who were incubated with scrambled shRNA (left) or PIEZO2 shRNA (right) lentivirus. (G) Summary data of PIEZO2 MA currents evoked with different membrane displacements at 20 min in scrambled shRNA group (black square, $n = 9$) or PIEZO2 shRNA group (red circle, $n = 10$) of 5 μmol/L VCR intracellularly treated DRG neurons. (H) Representative traces of PIEZO2 currents elicited by a set of membrane displacements from 1 to 10 μm (above the current traces) at the initial time (black traces) and 15−20 min (red traces) in control group (above the dish line) and in 5 μmol/L VCR intracellular treatment group (below the dish line, VCR) in PIEZO2 transfected HEK 293T cells. In VCR group, the grey traces represented PIEZO2 currents were extracellularly treated with 10 μmol/L D-GsMTx4 at 15−20 min. (I) Summary data of PIEZO2 currents evoked with different membrane displacements at 15−20 min in control group (black square, $n = 5$), VCR-treatment group (red circle, $n = 4$) and VCR + D-GsMTx4 group (grey triangle, $n = 5$) of PIEZO2 transfected HEK 293T cells. Data are shown in mean ± SEM; $^{\#/\$/*}P < 0.05$, $^{\#\#/\$\$/**}P < 0.01$, $^{\#\#\#/\$\$\$/***}P < 0.001$.

GsMTx4 (10 μmol/L), a specific PIEZO2 channel inhibitor[36], significantly suppressed VCR-induced potentiation of PIEZO2 currents in heterologous expression HEK 293T cells (Fig. 4H and I).

VCR treatment also led PIEZO2 MA currents to be more easily activated. The mechanical threshold for evoking PIEZO2 MA currents was significantly reduced by ∼45% following VCR application for 30 min ($n = 8$, $P < 0.05$, Fig. 5A and B). In contrast, there was no significant change in mechanical threshold in control group ($n = 16$, Fig. 5A and B). We then examined the onset latency for evoking PIEZO2 MA currents. The latency was no significant difference between initial time (6.3 ± 0.3 ms, $n = 11$) and 30 min following whole-cell configuration (5.3 ± 0.4 ms, $n = 20$) in the control group (Fig. 5C and E). In

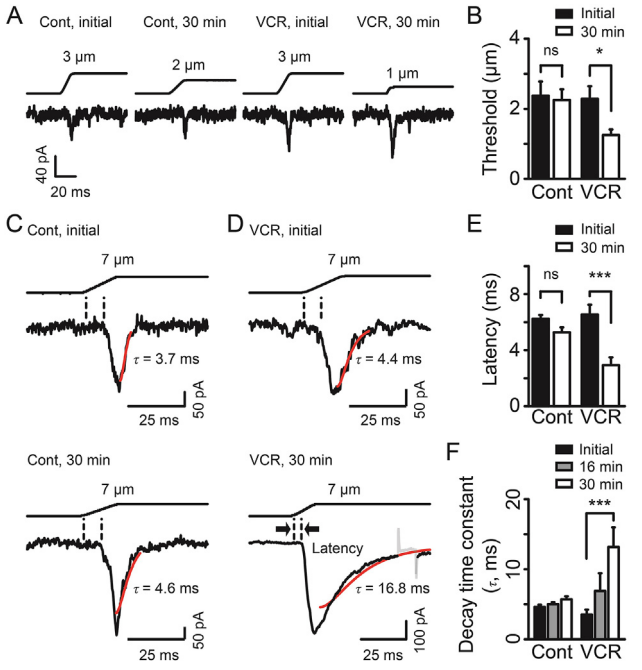

Figure 5 VCR treatment affected the properties of PIEZO2 MA currents. (A) Representative traces of PIEZO2 MA currents elicited by minimum membrane displacements at the initial time and 30 min after establishing whole-cell mode patch recordings with (VCR) or without (Cont) intracellular administration of VCR (5 μmol/L). (B) Mechanical thresholds for evoking PIEZO2 MA currents at initial time (solid bars) and 30 min (open bars) with (VCR) or without (Cont) intracellular administration of VCR. $n = 16$ (Cont initial), 16 (Cont 30 min), 9 (VCR initial) and 8 (VCR 30 min), respectively. Representative traces of PIEZO2 MA currents elicited by a 7-μm membrane displacement at the initial time (top) and 30 min (bottom) without (left, Cont) (C) or with (right, VCR) (D) VCR treatment. The inactivation kinetics were fitted with single exponential function (red line) and the decay time constants (τ) were shown. The interval between dash lines (bold arrow) show the onset latency for evoking PIEZO2 MA currents. (E) Summary of the latency for evoking PIEZO2 MA currents at initial time (solid bars) and 30 min (open bars) with (VCR) or without (Cont) VCR treatment. $n = 11$ (Cont initial), 20 (Cont 30 min), 15 (VCR initial) and 8 (VCR 30 min), respectively. (F) Summary of decay time constants of PIEZO2 MA currents at initial time (solid bars), 16 min (gray bars) and 30 min (open bars) with (VCR) or without (Cont) VCR treatment. $n = 39$ (Cont initial), 38 (Cont 16 min), 31 (Cont 30 min), 11 (VCR initial), 12 (VCR 16 min) and 11 (VCR 30 min), respectively. Data are shown in mean ± SEM; $^{*}P < 0.05$, $^{***}P < 0.001$, ns indicates no significant difference.

contrast, the onset latency in VCR treatment group was significantly reduced from 6.6 ± 0.7 ms ($n = 15$) at initial time to 2.9 ± 0.6 ms ($n = 8$, $P < 0.001$) at 30 min (Fig. 5D and E). VCR treatment also slowed the inactivation kinetics of PIEZO2 MA currents over time. For example, PIEZO2 MA currents had a decay time constant (τ) of 3.5 ± 0.7 ms at initial time ($n = 11$) and it prolonged to 13.2 ± 2.8 ms ($n = 11$, $P < 0.001$) at 30 min after VCR treatment (Fig. 5D and F). In contrast, there were no significant changes in the decay time constant in control group (Fig. 5C and F). Taken together, these results demonstrate that VCR significantly potentiates PIEZO2 MA currents in rat DRG neurons.

3.5. VCR mimics the effect of osmotic swelling on PIEZO2 MA currents in DRG neurons

We have previously shown that PIEZO2 MA currents in DRG neurons are potentiated by osmotic swelling through increasing SPMT[32]. We then compared the effects of VCR and osmotic swelling on cell size and PIEZO2 MA currents in DRG neurons. Cell diameters were measured after establishing whole-cell mode patch with hypertonic recording internal solution (420 mOsm) and isotonic recording solution that contained 5 μmol/L VCR. Similar to hypertonic internal solution-induced cell swelling, application of VCR resulted in DRG neuron swelling (Fig. 6A and B). For example, cell diameters increased by 25.2% ($n = 11$, $P < 0.01$) at 16 min and 35.9% ($n = 10$, $P < 0.001$) at 32 min after treatment with hypertonic internal solution (Fig. 6A). Similarly, cell diameters significantly increased by 10.3% ($n = 13$, $P < 0.001$) at 16 min and 21.2% ($n = 10$, $P < 0.001$) at 32 min after VCR treatment (Fig. 6B). Accompanied with the increased cell sizes, PIEZO2 MA currents were significantly potentiated by hypertonic internal solution (Fig. 6C and D), furthermore, the potentiation effects were rapidly abolished when osmotic gradient was canceled out following the application of hypertonic bath solution at the osmolarity of 420 mOsm (Fig. 6C and D). Similarly, accompanied with the cell swelling induced by VCR, PIEZO2 MA currents were significantly enhanced following VCR treatment. Interestingly, the potentiation effect on PIEZO2 MA currents induced by VCR was abolished following the application of hypertonic bath solution (420 mOsm) (Fig. 6E and F).

The onset latency of PIEZO2 MA currents was 6.1 ± 0.5 ms ($n = 21$) at initial time of establishing the whole-cell mode patch and significantly shortened to 2.4 ± 0.2 ms ($n = 21$, $P < 0.001$) at 30 min by hypertonic internal solution-induced cell swelling (Fig. 7A and C). Similarly, the onset latency of PIEZO2 MA currents was 5.8 ± 0.8 ms ($n = 10$) at initial time of establishing the whole-cell mode patch and significantly shortened to 2.9 ± 0.6 ms ($n = 8$, $P < 0.05$) at 30 min by VCR treatment (Fig. 7B and C). After introducing the hypertonic bath solution, the shortened onset latencies are dramatically prolonged to 5.9 ± 1.1 ($n = 7$, $P < 0.001$) and 6.0 ± 0.9 ms ($n = 5$, $P < 0.01$), respectively (Fig. 7A–C). The decay time constant was 4.9 ± 0.5 ms ($n = 15$) at initial time of establishing the whole-cell mode patch and significantly slowed to 29.5 ± 4.1 ms ($n = 20$, $P < 0.001$) at 30 min by hypertonic internal solution-induced cell swelling (Fig. 7A and D). Similarly, the decay time constant was 2.8 ± 0.5 ms ($n = 11$) at initial time and significantly slowed to 13.2 ± 2.8 ms ($n = 11$, $P < 0.01$) at 30 min by VCR treatment (Fig. 7B and D). After introducing the hypertonic bath solution, the slowed decay time constants were accelerated to 3.0 ± 1.2 ($n = 7$, $P < 0.001$) and 3.6 ± 0.6 ms ($n = 5$, $P < 0.05$), respectively (Fig. 7A, B and D). Taken together, these results suggest that the potentiation of PIEZO2 MA currents in DRG neurons induced by both VCR and osmotic swelling may share the same mechanism.

3.6. VCR potentiates PIEZO2 MA currents through increasing SPMT of DRG neurons

Our previous study has demonstrated that osmotic swelling-induced potentiation of PIEZO2 MA currents was due to the increased SPMT in rat DRG neurons[32]. We then examined whether VCR treatment affects the SPMT of DRG neurons. Using the micropipette aspiration method, SPMT of DRG neurons was measured[32,33]. In this set of experiments, VCR (5 μmol/L) was delivered

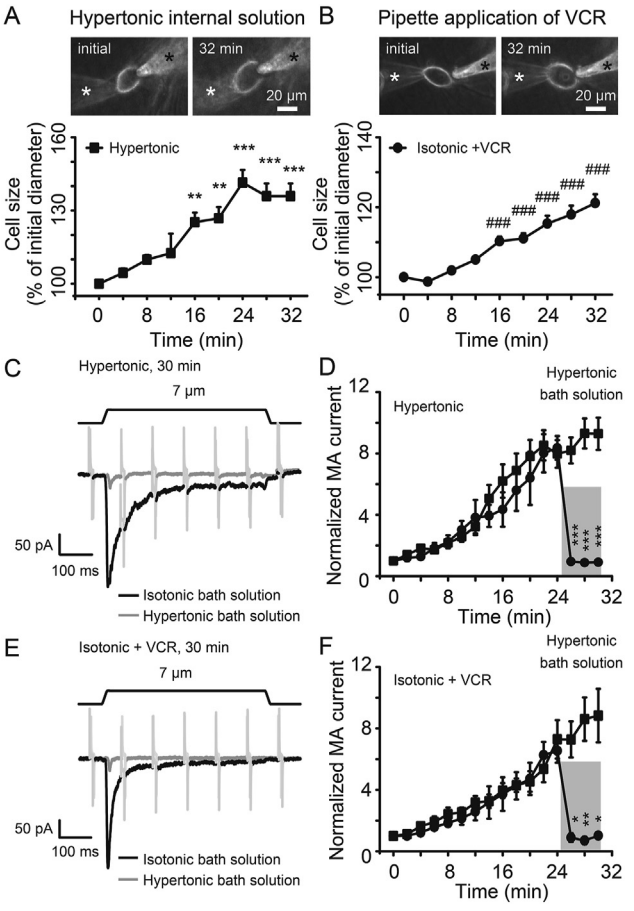

Figure 6 VCR mimicked the effects of osmotic swelling on PIEZO2 MA currents in DRG neurons. Images (top) and time courses (bottom) of cell swelling induced by hypertonic internal solution (420 mOsm, $n = 10$) (A) and pipette application of VCR (5 μmol/L, $n = 10$) (B) after establishing the whole-cell mode patch recording over time. The position of the recording electrode and mechanical stimulation probe are indicated by a white and a black star, respectively. (C) Sample traces show PIEZO2 MA currents at 30 min after establishing whole-cell mode patch recording with hypertonic internal solution (420 mOsm). At that time, cells were perfused with isotonic bath solution (black line) or hypertonic bath solution (420 mOsm, gray line). Membrane displacement was 7 μm (above). (D) Summary data of the potentiation of PIEZO2 MA currents over time using hypertonic internal solution (Hypertonic). In the last 6 min, cells were perfused with isotonic bath solution ($n = 14$) and hypertonic bath solution (420 mOsm, gray stripe, $n = 5$), respectively. (E) Similar to (C) but the sample traces of PIEZO2 MA currents were recorded using isotonic internal solution containing 5 μmol/L VCR (Isotonic + VCR). (F) Summary data of the potentiation of PIEZO2 MA currents over time using isotonic internal solution contained 5 μmol/L VCR (Isotonic + VCR). In the last 6 min, cells were perfused with isotonic bath solution ($n = 10$) and hypertonic bath solution (420 mOsm, gray stripe, $n = 4$), respectively. Data are shown in mean ± SEM; $^{*}P < 0.05$, $^{**}P < 0.01$, $^{***/\#\#\#}P < 0.001$.

intracellularly *via* the whole-cell patch-clamp recording electrode (Fig. 8A). Under the isotonic condition, SPMT was 24 ± 1 mN/mm ($n = 8$) at baseline and did not significantly change over time after establishing the whole-cell mode patch (Fig. 8B). In contrast, SPMT was significantly increased from a baseline SPMT of 23 ± 1 mN/mm

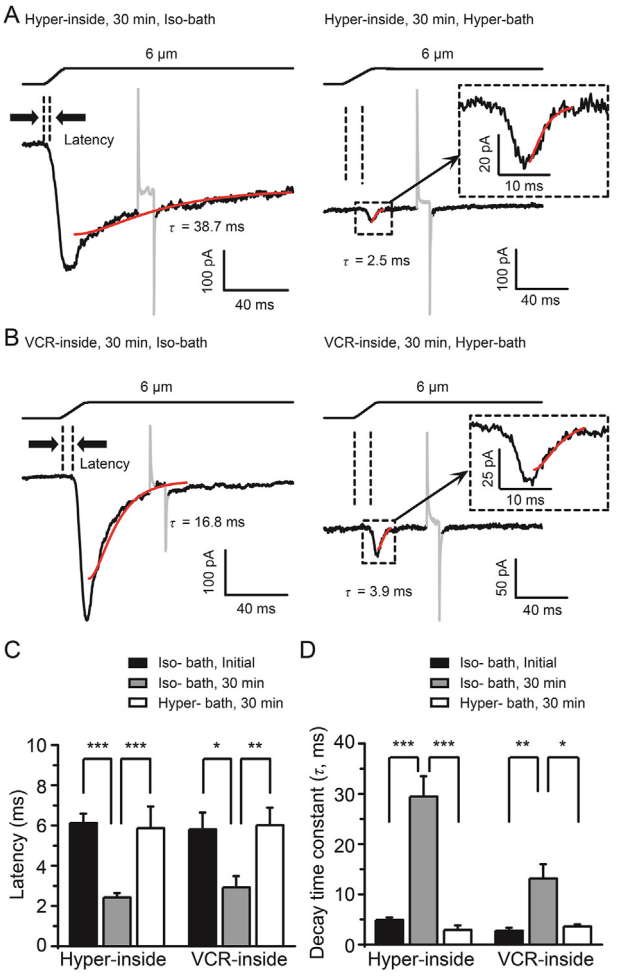

Figure 7 The VCR-induced changes in the properties of PIEZO2 MA currents were reversed by hypertonic bath solution. (A) Representative traces of PIEZO2 MA currents elicited by a 6-μm membrane displacement at 30 min (bottom) after establishing whole-cell mode patch recording with hypertonic internal solution (420 mOsm) (Hyper-inside) and isotonic bath solution (left, Iso-bath) or hypertonic bath solution (right, 420 mOsm) (Hyper-bath). (B) Representative traces of PIEZO2 MA currents elicited under the same conditions as in (A) but recorded with isotonic internal solution containing 5 μmol/L VCR (VCR-inside). In (A) and (B), the onset latency for evoking PIEZO2 MA currents is indicated by dish lines, the inactivation kinetics are fitted with a single exponential function (red line) and the decay time constants (τ values) are shown. Insets in the right panels in (A) and (B), extended scale for the boxed region is shown. Summary data of the latency (C) and decay time constants (τ) (D) of PIEZO2 MA currents under the above conditions are shown. Hypertonic bath solution (Hyper-bath) reversed the changes in the properties of PIEZO2 MA currents induced by osmotic swelling (Hyper-inside) and VCR (VCR-inside). Data are shown in mean ± SEM, $n = 21$ and 15 (Hyper-inside, Iso-bath, initial), 21 and 20 (Hyper-inside, Iso-bath, 30 min), 7 and 7 (Hyper-inside, Hyper-bath, 30 min), 10 and 11 (VCR-inside, Iso-bath, initial), 8 and 11 (VCR-inside, Iso-bath, 30 min) and 5 and 5 (VCR-inside, Hyper-bath, 30 min) in (C) and (D), respectively; $^{*}P < 0.05$, $^{**}P < 0.01$, $^{***}P < 0.001$.

($n = 8$) to 28 ± 2 mN/mm at 2.5 min ($n = 8$), 39 ± 3 mN/mm at 17.5 min ($n = 8$, $P < 0.05$) and 57 ± 7 mN/mm at 32.5 min ($n = 8$, $P < 0.01$) after VCR treatment (Fig. 8B). As a positive control,

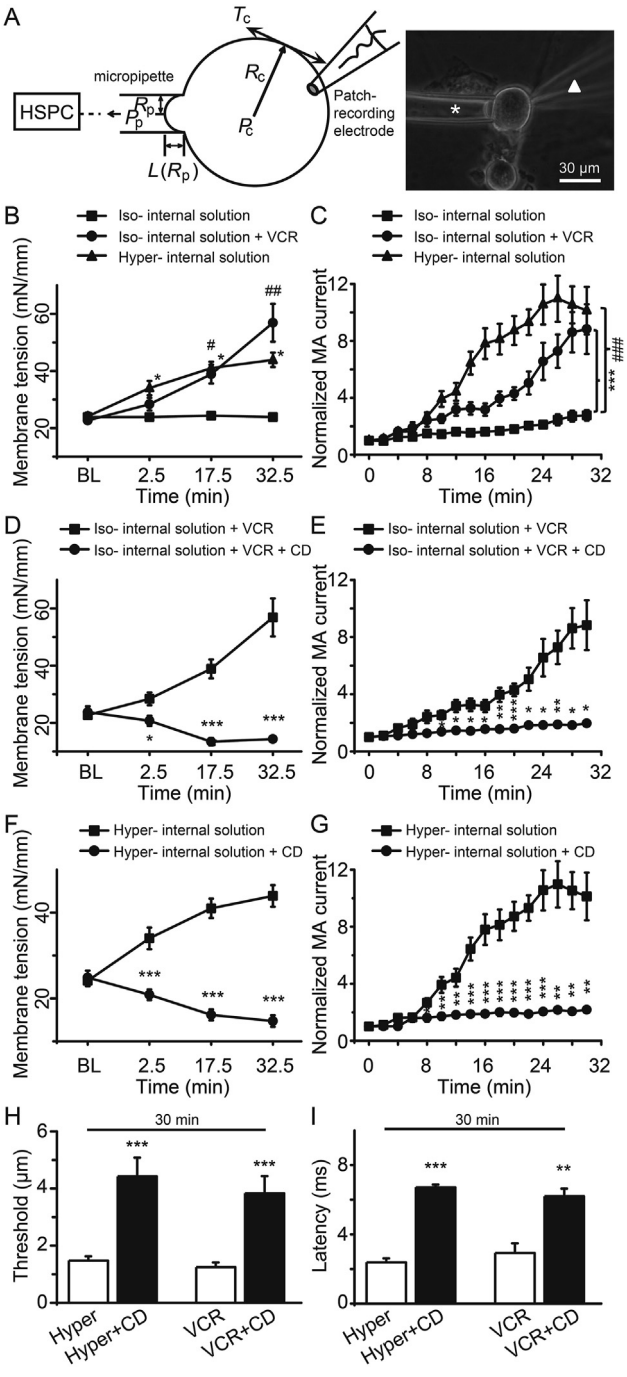

Figure 8 Increment of SPMT mediated VCR-induced potentiation of PIEZO2 MA currents in DRG neurons. (A) Model for measuring SPMT using a micropipette aspiration technique. Stepwise negative pressures were generated by HSPC and delivered to the micropipette to aspirate a cell. Parameters needed for calculating membrane tension based on the Young−Laplace equation are shown in left panel. T_c, membrane tension; R_c, cell radius; P_c, intracellular pressure; P_p, pipette aspiration pressure; R_p, pipette radius; L, length of membrane. An image shows a DRG neuron whose membranes are being aspirated into the micropipette (white asterisk). The cell is also patched under the whole-cell mode patch by a recording electrode (white triangle) that contains different recording internal solution. (B) The SPMT was measured over time under the whole-cell mode patch recording with isotonic internal solution (square, $n = 8$), isotonic internal solution containing 5 μmol/L VCR (circle, $n = 8$) and hypertonic internal solution (420 mOsm, triangle, $n = 9$). BL, baseline before establishing the whole-cell mode patch. (C) PIEZO2 MA currents were recorded from DRG neurons over time under the conditions in (B). $n = 17$, 10 and 13, respectively. The SPMT (D) and PIEZO2 MA currents (E) were measured from DRG neurons over time with (circle, $n = 7$) or without (square, $n = 8$) adding 10 μmol/L CD to the isotonic internal solution containing VCR. The SPMT (F) and PIEZO2 MA currents (G) were measured from DRG neurons over time with (circle, $n = 7$) or without (square, $n = 9$) adding CD (10 μmol/L) to the hypertonic internal solution. The mechanical thresholds (H) and the onset latency (I) for evoking PIEZO2 MA currents at 30 min after establishing whole-cell mode patch recording with hypertonic internal solution (Hyper), or hypertonic internal solution containing CD (Hyper + CD), or isotonic internal solution containing VCR (VCR) or isotonic internal solution containing VCR and CD (VCR + CD) were measured. $n = 27$ (Hyper), 8 (Hyper + CD), 8 (VCR) and 6 (VCR + CD) in (H); $n = 16$ (Hyper), 5 (Hyper + CD), 8 (VCR) and 5 (VCR + CD) in (I), respectively. Data are shown in mean ± SEM; $^{*/\#}P < 0.05$, $^{**/\#\#}P < 0.01$, $^{***/\#\#\#}P < 0.001$.

hypertonic internal solution (420 mOsm)-induced osmotic swelling significantly increased the SPMT at different time points (Fig. 8B). Accompanied with the significant increases of SPMT, PIEZO2 MA currents were also gradually increased either following VCR treatment or hypertonic internal solution-induced osmotic swelling (Fig. 8C). We used CD, a disruptor of actin filament who can reduce the SPMT of DRG neurons[32,37] and we found that CD counteracted SPMT increment induced either by VCR or by hypertonic internal solution (Fig. 8D and F). Compared with the VCR group, CD (10 μmol/L) significantly reduced the SPMT values to 21 ± 2 mN/mm at 2.5 min ($n = 7$, $P < 0.05$), 13 ± 1 mN/mm at 17.5 min ($n = 7$, $P < 0.001$) and 14 ± 1 mN/mm at 32.5 min ($n = 7$, $P < 0.001$), respectively (Fig. 8D). Consistent with the reduction of SPMT, VCR-induced potentiation of PIEZO2 MA currents was also significantly inhibited by CD in DRG neurons (Fig. 8E). As a positive control, CD counteracted osmotic swelling-induced increment of SPMT and potentiation of PIEZO2 MA currents in DRG neurons (Fig. 8F and G). The mechanical threshold for evoking PIEZO2 MA currents was 1.3 ± 0.2 μm ($n = 8$) following VCR treatment for 30 min. When CD was co-applied with VCR for 30 min, the mechanical threshold significantly increased to 3.8 ± 0.6 μm ($n = 6$, $P < 0.001$) (Fig. 8H). The onset latency for evoking PIEZO2 MA currents was 2.9 ± 0.6 ms ($n = 8$) with VCR application for 30 min, while it significantly increased to 6.2 ± 0.4 ms ($n = 5$, $P < 0.01$) when CD was co-applied with VCR for 30 min (Fig. 8I). Similarly, CD counteracted the reduced mechanical threshold and shortened onset latency that was induced by hypertonic internal solution (Fig. 8H and I). These results indicate that VCR potentiates PIEZO2 MA currents may be due to increasing SPMT in DRG neurons.

3.7. Disruption but not stabilization of microtubules potentiates PIEZO2 MA currents in rat DRG neurons

VCR is a commonly used disruptor of microtubules, which prevents tubulin polymerization from soluble dimers. To determine the role of microtubules in the modulation of PIEZO2 MA currents, we examined the effects of nocodazole (NDZ) and paclitaxel (TAXEL) on PIEZO2 MA currents in cultured rat DRG neurons. Similar to VCR, NDZ functions as a disruptor of

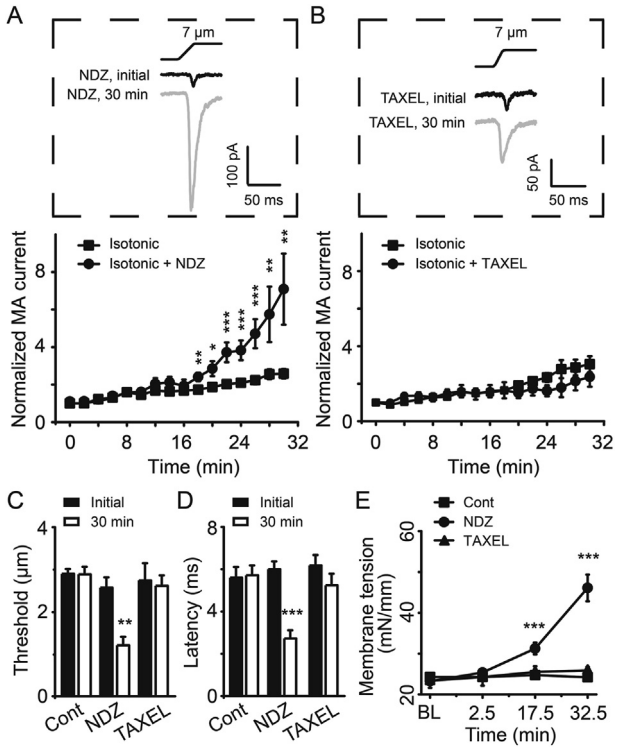

Figure 9 Disruption but not stabilization of microtubules potentiated PIEZO2 MA currents in DRG neurons. Sample traces (top) and time courses (bottom) of PIEZO2 MA currents evoked by a 7-μm membrane displacement after establishing whole-cell mode patch recording with isotonic internal solution containing 5 μmol/L NDZ (A) or 1 μmol/L TAXEL (B) over time. In the top panels in (A) and (B), the traces of PIEZO2 MA currents at the initial time and 30 min are indicated with black line and gray line, respectively. $n = 14$ (Isotonic) and 8 (Isotonic + NDZ) in (A); $n = 13$ (Isotonic) and 9 (Isotonic + TAXEL) in (B), respectively. The mechanical thresholds (C) and the onset latency (D) for evoking PIEZO2 MA currents at initial time (solid bars) and 30 min (open bars) after establishing whole-cell mode patch recording with isotonic internal solution (Cont), or isotonic internal solution containing NDZ (NDZ) or isotonic internal solution containing TAXEL (TAXEL) were measured. $n = 9$ (Cont initial), 7 (Cont 30 min); $n = 9$ and 9 (NDZ initial), 6 and 8 (NDZ 30 min), 11 and 9 (TAXEL initial) and 6 and 8 (TAXEL 30 min) in (C) and (D), respectively. (E) The SPMT was measured over time among the above 3 groups of DRG neurons (square, Cont, $n = 11$; circle, NDZ, $n = 8$; and triangle, TAXEL, $n = 8$). BL, baseline before establishing the whole-cell mode patch. Data are shown in mean ± SEM; $*P < 0.05$, $**P < 0.01$, $***P < 0.001$.

microtubules, while TAXEL functions as a stabilizer of microtubules[37,38]. NDZ (5 μmol/L) or TAXEL (1 μmol/L) were directly administrated into DRG neurons through the isotonic recording pipette solution. The amplitude of PIEZO2 MA currents was gradually but significantly increased following NDZ application (Fig. 9A). For example, following NDZ treatment the amplitudes of PIEZO2 MA currents increased to 2.4-fold ($n = 8$, $P < 0.01$) at 18 min, 3.8-fold ($n = 8$, $P < 0.001$) at 24 min and about 7.1-fold ($n = 8$, $P < 0.01$) at 30 min (Fig. 9A). Whereas, following TAXEL treatment the PIEZO2 MA currents in DRG neurons did not significantly change over time compared with control group (Fig. 9B). NDZ treatment resulted in a significant reduction of mechanical threshold for evoking PIEZO2 MA currents from 2.6 ± 0.2 μm ($n = 9$) at initial time to 1.2 ± 0.2 μm ($n = 6$, $P < 0.01$) at 30 min in DRG neurons (Fig. 9C). In contrast, there was no significant difference in mechanical threshold between initial time (2.7 ± 0.4 μm, $n = 11$) and 30 min (2.6 ± 0.2 μm, $n = 6$; $P > 0.05$) following TAXEL application (Fig. 9C). Similarly, following NDZ treatment the onset latency was shortened from 6.0 ± 0.4 ms ($n = 9$) at initial time to 2.7 ± 0.4 ms ($n = 8$, $P < 0.001$) at 30 min (Fig. 9D). In contrast, TAXEL treatment did not change the onset latency over time (6.2 ± 0.5 ms, $n = 9$, initial time *vs.* 5.2 ± 0.5, $n = 8$, 30 min; $P > 0.05$) (Fig. 9D). Furthermore, we found that the SPMT significantly increased to 31 ± 1 mN/mm ($n = 8$, $P < 0.001$) at 17.5 min and 46 ± 3 mN/mm ($n = 8$, $P < 0.001$) at 32.5 min from the baseline of 23 ± 6 mN/mm ($n = 8$) following NDZ treatment (Fig. 9E). While TAXEL treatment did not induce any obvious changes in the SPMT of DRG neurons over time (Fig. 9E). Be consistent with the effects on PIEZO2 MA currents, NDZ but not TAXEL induced DRG neurons small but significant cell swelling by measuring their diameters (Supporting Information Fig. S4). These results indicate that disruption but not stabilization of microtubules would increase the SPMT hence potentiate PIEZO2 MA currents in rat DRG neurons.

Noticing that these chemotherapeutic drugs were usually on the basis of extracellular administration in clinic, we then examined the effects of VCR, NDZ and TAXEL on PIEZO2 MA currents in DRG neurons through extracellular application. Similarly, incubation of DRG neurons with VCR (5 μmol/L) or NDZ (5 μmol/L) for 1 h, PIEZO2 MA currents were dramatically potentiated, while incubation of TAXEL (1 and 5 μmol/L) for 1 h showed no effects on PIEZO2 MA currents in DRG neurons (Supporting Information Fig. S5). Taken together, these results further determined the potentiation effects of VCR on PIEZO2 MA currents. We also examined the effects of VCR, NDZ and TAXEL on PIEZO2 expression in DRGs. As shown in Supporting Information Fig. S6, incubation of DRGs for 1 h by VCR significantly reduced the expression of PIEZO2 while 1 h incubation with NDZ or TAXEL showed no significant changes in PIEZO2 expression (Supporting Information Fig. S6A and S6B). Interestingly, incubation of DRGs with hypotonic solution (220 mOsm) for 30 min significantly increased the expression of PIEZO2 (Fig. S6C and S6D), which was consistent with the effect of hypotonic solution potentiating PIEZO2 MA currents through enhancing SPMT in DRG neurons[32].

3.8. DRG neurons of VCR-induced neuropathic pain rats show potentiated PIEZO2 MA currents and elevated SPMT

We next recorded PIEZO2 MA currents from acutely dissociated DRG neurons of VCR-induced neuropathic pain model rats. We also measured the SPMT of these DRG neurons to determine whether rats treated with VCR will result in a change of SPMT in their DRG neurons. We found that DRG neurons from VCR-pain model rats have larger PIEZO2 MA currents in comparison with those of control groups (Fig. 10A and B). For example, tested with a 7-μm membrane displacement, the PIEZO2 MA current density showed ~4-fold higher in DRG neurons of VCR-pain model rats than those of control group (Fig. 10A and B). Incubated the DRG neurons of VCR-pain model rats with CD, their PIEZO2 MA currents could be greatly reduced to control level (Fig. 10A and B). In addition, DRG neurons from VCR-pain model rats have

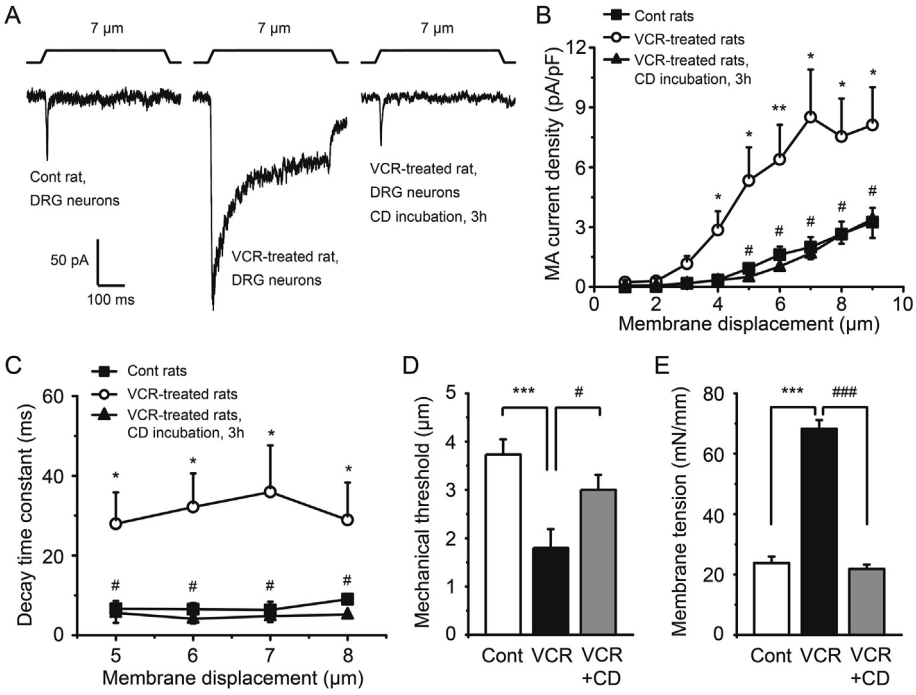

Figure 10 VCR-induced pain model rats showed potentiated PIEZO2 MA currents and elevated SPMT in their DRG neurons. (A) Three sample traces showed the PIEZO2 MA currents evoked by a 7-μm membrane displacement in DRG neurons of control rats (left), VCR-induced pain model rats (middle) and VCR-pain model rats but their neurons were incubated with 10 μmol/L CD for 3 h (right), respectively. (B) Summary data of the PIEZO2 MA current densities in the above three groups of DRG neurons (n = 14, 11 and 7, respectively). (C) The decay time constants of PIEZO2 MA currents were measured from the above three groups of DRG neurons (n = 7, 6 and 6, respectively) at different membrane displacement stimulus (5- to 8-μm). The mechanical thresholds (D) and the SPMT (E) were measured among the above three groups of DRG neurons. VCR-induced pain model rats showed potentiated PIEZO2 MA currents and elevated SPMT in their DRG neurons and these could be reduced by CD. n = 15, 10 and 7 in (D); n = 16, 9 and 11 in (E), respectively. Data are shown in mean ± SEM; $^{*/\#}P < 0.05$, $^{**}P < 0.01$, $^{***/\#\#\#}P < 0.001$.

significantly slower decay time constants in comparison with that of control rats (Fig. 10C). For example, they have a slow decay time constant of 35.9 ± 11.7 ms (n = 6), which was slower than that of 6.4 ± 2.1 ms (n = 7, $P < 0.05$) in control group when the DRG neurons were tested with a 7-μm membrane displacement (Fig. 10C). Incubated the DRG neurons of VCR-pain model rats with CD, the decay time constants were significantly reduced to control levels (*e.g.*, 4.8 ± 0.4 ms, n = 6, $P < 0.05$; 7-μm membrane displacement) (Fig. 10C). Tested with 7-μm membrane displacement stimulation, the mechanical threshold for evoking PIEZO2 MA currents in DRG neurons of VCR-pain model rats was 1.8 ± 0.4 μm (n = 10), which was significantly lower than that of control group (3.7 ± 0.3 μm, n = 15; $P < 0.001$). Incubation of these DRG neurons with CD significantly decreased the mechanical threshold to 3.0 ± 0.3 μm (n = 7, $P < 0.05$) (Fig. 10D). Consistently, DRG neurons from VCR-pain model rats had a significantly higher SPMT (68 ± 3 mN/mm, n = 9, $P < 0.001$) compared with that of control group (24 ± 2 mN/mm, n = 16). The SPMT of the DRG neurons from VCR-pain model rats was significantly reduced (22 ± 2 mN/mm, n = 11, $P < 0.001$) when these DRG neurons were incubated with CD (Fig. 10E).

4. Discussion

The major findings of the present study are as follows: i) VCR dramatically potentiates PIEZO2 MA currents through increasing SPMT in rat DRG neurons; ii) Reduction of SPMT, or knocking down the expression of PIEZO2 channel, or blocking PIEZO2 MA channel activities, significantly suppresses VCR-induced mechanical allodynia and hyperalgesia; iii) VCR-induced potentiation of PIEZO2 MA currents in rat DRG neurons is not due to the elevated expression of PIEZO2. The present study has shown that VCR-induced potentiation of PIEZO2 MA currents through increasing SPMT in DRG neurons may play an essential role in mediating VCR-induced mechanical hypersensitivity. These findings may also have several clinical implications. First, PIEZO2 may potentially serve as a therapeutic target for eliminating VCR-induced mechanical hypersensitivity. Second, the reduction of SPMT may use as an alternative option to eliminate VCR-induced mechanical hypersensitivity under the condition that no selective and safe inhibitor of PIEZO2 channel has been found yet. Third, the development of small molecules that selectively inhibit PIEZO2 may be a useful pharmacological intervention for the treatment of VCR-induced mechanical hypersensitivity.

One key observation in the present study is that the potentiation of PIEZO2 MA channel activity contributes to VCR-induced mechanical hypersensitivity. Either inhibition of PIEZO2 channel by Gd^{3+} or focal knockdown of PIEZO2 in DRG neurons by shRNA interference eliminated VCR-induced mechanical allodynia and hyperalgesia. Furthermore, sensory neuron-specific knockdown of PIEZO2 significantly increased the touch threshold. PIEZO2 rather than acid-sensing ion channels or transient receptor potential

channels as *bona fide* class of mammalian MA channel that dominantly expressed in primary sensory neurons and cutaneous Merkel cells. It has been confirmed that PIEZO2 is essentially required for the formation of gentle touch sensation[16,21−24]. In sensory neurons, PIEZO2 mediating RA MA currents is expressed in more than 95% of low-threshold mechanoreceptors, ∼90% of isolectin B_4-positive non-peptidergic nociceptors, ∼70% of calcitonin gene-related peptide-positive peptidergic nociceptors, and 76% of high-threshold mechanoreceptors[16,25,39]. In addition, PIEZO2 also mediates intermediately adapting even slowly adapting MA currents in nociceptive DRG neurons when they are subjected to nerve growth factor treatment, although in normal condition these nicotinic acetylcholine receptor subunit alpha-3-positive nociceptive DRG neurons expressing PIEZO2 are "silence" to mechanical stimulation[40]. These previous studies have shown that PIEZO2 extensively distributes in sensory neurons and actively responds to inflammatory conditions. Studies on either sensory neuron-specific PIEZO2 knockout mice or human patients with loss of function mutations in *PIEZO2* gene have demonstrated that inhibition of PIEZO2 results in gentle touch impaired, loss of two points discrimination and suppression of peripheral nerve injury-induced mechanical allodynia and hyperalgesia[22,27−29]. Focal knockdown of DRG PIEZO2 by antisense, not only suppresses peripheral nerve damage-induced mechanical allodynia but also increases the touch threshold[41]. Combined with our observation, these studies strongly suggest that PIEZO2 may account for the light touch sensation in physiology and mechanical hypersensitivity in pathology, respectively. However, Zhang et al.[25] described more recently that DRG neurons-conditional knockout of PIEZO2 induced downregulation of nociceptive withdrawal threshold, which indicates that PIEZO2 may have a role in suppression of mechanical pain (mechanical hyperalgesia determined by Randall−Selitto test). One possibility is that PIEZO2-mediated touch may suppress pressure-induced mechanical hyperalgesia under normal condition but great potentiation of PIEZO2 MA channel activity under pathological conditions such as inflammation or nerve injury may mediate or sensitize mechanical hyperalgesia[29,40]. In the present study, knockdown of PIEZO2 by shRNA interference significantly elevates the thresholds in von Frey test while showing no changes in nociceptive thresholds in Randall−Selitto test when compared to the normal level. Knockdown of PIEZO2 certainly inhibits its role, as the light touch receptor[22,23,25], resulting in touch retardation so the thresholds are increased to high level even overcome the effects of VCR. Whereas knockdown of PIEZO2 also relieves its role in suppression of mechanical pain (Randall−Selitto model)[25] so the nociceptive thresholds should not be increased or be even decreased. To date, the nociceptive mechanoreceptors (pressure receptors) have not been clearly determined. Further researches for the identification of the molecular basis of nociceptive mechanoreceptors and its functional modulation are required in the future.

Another key observation in the present study is that increasing SPMT of DRG neurons may mediate VCR-induced potentiation of PIEZO2 MA currents and mechanical hypersensitivity. Membrane tension model (force-from-lipids model) played a key role in modulation of MA channels including PIEZO channels[17,18]. Stomatin-like protein 3 (STOML3) was reported to interact with PIEZO2 channel and facilitate PIEZO2 MA currents in co-expressing heterologous system[42,43]. STOML3 facilitating PIEZO2 MA currents is due to increasing membrane tension by recruiting membrane cholesterol[42,43]. Our previous study provided further evidence that osmotic swelling remarkably potentiated PIEZO2 MA currents through increasing SPMT in rat DRG neurons[32]. Reduction of SPMT by CD, not only reduced the osmotic swelling-induced potentiation of PIEZO2 MA currents in rat DRG neurons but also eliminated the osmotic swelling-induced mechanical hypersensitivity in rats[32]. Similar to the swelling effect on DRG neurons produced by intracellular hypertonic osmolarity, VCR application also induced swelling of DRG neurons in the present study. This notion has been supported by previous observations that VCR significantly induced swelling of primary afferent axon as well as sensory neurons in spinal ganglion[44,45]. Besides, either VCR-treated DRG neurons or DRG neurons isolated from VCR-pain model rats, have a significantly high level of SPMT. Reduction of SPMT of DRG neurons by CD, or application of hypertonic bath solution to reverse the osmotic gradient between intracellular and extracellular sides of DRG neurons, both abolished VCR-induced potentiation of PIEZO2 MA currents. More importantly, CD treatment eliminated VCR-induced mechanical hypersensitivity. These findings strongly support that the possible mechanism of VCR-induced potentiation of PIEZO2 MA currents through increasing SPMT of DRG neurons, which plays a crucial role in mediating VCR-induced mechanical allodynia and hyperalgesia. On the other hand, the possibility of tether proteins model (force-from-filaments model)[17] in the modulation of PIEZO2 MA channel cannot be completely excluded. For example, STOML3 is expressed in sensory neurons of mammals. It is a mammalian homologue of MEC-2, a tether protein that link MA channel to the cytoskeleton in *Caenorhabditis elegans*[46,47]. RA MA channel in DRG neurons was reported to be linked to the extracellular matrix through a ∼100 nm length protein filament[48]. Further investigation into the possibility of PIEZO2 linking with tether proteins is required.

The present study mentioned the possibility that VCR may induce PIEZO2 trafficking from cytoplasm to the membrane in DRG neurons. If this idea holds true, it could be another possible mechanism by which VCR potentiated PIEZO2 MA currents. Then, immunostaining assay was performed to test this preliminary idea. We first measured the IF of PIEZO2 in DRG sections in VCR-pain model rats and control rats. Indeed, the IF of PIEZO2 was uniformly distributed in DRG neurons in control rats, whereas the PIEZO2 IF was concentrated in cell membrane but relatively reduced in cytoplasm in DRG neurons in VCR-pain model rats (Supporting Information Fig. S7A). The PIEZO2 IF ratio of cell membrane to cytoplasm was significantly increased in VCR-pain model rats than that in control rats (Fig. S7B). We then measured the PIEZO2 IF in VCR-treated cultured DRG neurons with immunostaining assay. Incubation of VCR (5 μmol/L) for 1 h induced obvious membrane trafficking in cultured DRG neurons (Fig. S7C). The IF of PIEZO2 along a line which crossed the cell showed an increase in membrane but a decrease in cytoplasm (Fig. S7C and S7D). While the PIEZO2 IF along the crossing line over cells was stable and uniform in cell membrane and cytoplasm in control DRG neurons (Fig. S7C and S7D). Hence, VCR-induced membrane trafficking of PIEZO2 may be contributed to VCR-induced potentiation of PIEZO2 currents in DRG neurons. Here we just discussed the preliminary idea and data of VCR-induced membrane trafficking of PIEZO2. To verify this mechanism, further investigation is needed in the future.

Several cytoskeleton-targeting agents used in the present study determined the contribution of cytoskeleton to membrane tension

and PIEZO2 MA current modulation. To our surprise, VCR or NDZ enhances SPMT hence potentiates PIEZO2 MA currents in rat DRG neurons. In contrast, TAXEL functioning as the stabilizer of microtubules has no effect on SPMT and PIEZO2 MA currents. It has been shown in previous studies that CD significantly reduces SPMT and inhibits PIEZO2 MA currents by disrupting actin filaments in rat DRG neurons[32,49]. CD also reduces the VCR-induced enhancement of SPMT and PIEZO2 MA currents in the present study. These data intensively indicate that membrane−cytoskeleton interaction significantly contributes to plasma membrane mechanics and PIEZO2 MA current modulation. The effect of CD on SPMT has been reported previously[49,50]. However, the effect of microtubules disruptor VCR or NDZ on SPMT in the present study is somehow inconsistent with previous studies. For example, VCR markedly increased the deformability of human platelets which was evaluated by micropipette aspiration[51]; NDZ significantly increased the tether length of chick embryo fibroblasts or T3 fibroblasts which was measured by Laser tweezers manipulation[49]. These results indicate that VCR or NDZ has the potential function of reducing membrane tension, although direct evidence is lacking. An analogue of VCR, vinblastine increased membrane tension by 40% in HeLa cells which were measured by Laser tweezers manipulation[52]. But vinblastine was used at a very low concentration of 2 nmol/L that only arrest cell cycle without causing depolymerization of microtubules[52]. Besides, previous studies have shown the opposite effects of VCR and TAXEL on PIEZO2 MA currents in mouse Merkel cells[53,54]. Combined with the effects of VCR on cell size and swelling in the present study and previous study[45], further research about the different effects of microtubule modulators on membrane mechanics and PIEZO2 MA currents in different cells and the underlying mechanisms are necessary.

5. Conclusions

We propose a hypothesis that VCR application leads to the swelling of DRG neurons and increasing their SPMT, which results in the potentiation of PIEZO2 MA currents thereby mediates VCR-induced mechanical hypersensitivity. Our findings strongly suggest that PIEZO2 may serve as a novel therapeutic target for relieving VCR-induced mechanical neuropathy.

Acknowledgments

This work was supported by NSFC grant 81571080 (Zhanfeng Jia, China), 81872848 (Wei Zhang, China); the Central Government Guiding Local Funding Project for Scientific and Technological Development 206Z7703G (Zhanfeng Jia, China); Key Project and Cultivation Project of Precision Medicine Joint Fund of Natural Science Foundation of Hebei Province H2021206406 (Zhanfeng Jia, China), H2022206211 (Wei Zhang, China) and H2020206165 (Zhanfeng Jia, China); Science and Technology Project of Hebei Education Department ZD2020107 (Zhanfeng Jia, China); Science Fund for Creative Research Groups of Natural Science Foundation of Hebei Province H2020206474, China.

Author contributions

Zhanfeng Jia designed the research. Mingli Duan, Yurui Jia, Lifang Huo, YitingGao, Jia Wang and Wei Zhang performed the research. Mingli Duan, Yurui Jia, Lifang Huo and Zhanfeng Jia analysed the data. Zhanfeng Jia wrote the manuscript.

Conflicts of interest

The authors declare no conflicts of interest.

Appendix A. Supporting information

Supporting data to this article can be found online at https://doi.org/10.1016/j.apsb.2023.05.010.

References

1. Sandler SG, Tobin W, Henderson ES. Vincristine-induced neuropathy. A clinical study of fifty leukemic patients. *Neurology* 1969;**19**:367−74.
2. Holland JF, Scharlau C, Gailani S, Krant MJ, Olson KB, Horton J, et al. Vincristine treatment of advanced cancer: a cooperative study of 392 cases. *Cancer Res* 1973;**33**:1258−64.
3. Himes RH, Kersey RN, Heller-Bettinger I, Samson FE. Action of the vinca alkaloids vincristine, vinblastine, and desacetyl vinblastine amide on microtubules *in vitro*. *Cancer Res* 1976;**36**:3798−802.
4. Owellen RJ, Hartke CA, Dickerson RM, Hains FO. Inhibition of tubulin−microtubule polymerization by drugs of the *Vinca* alkaloid class. *Cancer Res* 1976;**36**:1499−502.
5. Sisignano M, Baron R, Scholich K, Geisslinger G. Mechanism-based treatment for chemotherapy-induced peripheral neuropathic pain. *Nat Rev Neurol* 2014;**10**:694−707.
6. Weiden PL, Wright SE. Vincristine neurotoxicity. *N Engl J Med* 1972;**286**:1369−70.
7. Staff NP, Grisold A, Grisold W, Windebank AJ. Chemotherapy-induced peripheral neuropathy: a current review. *Ann Neurol* 2017;**81**:772−81.
8. Wang X, Li C, Wang Y, Chen H, Zhang X, Luo C, et al. Smart drug delivery systems for precise cancer therapy. *Acta Pharm Sin B* 2022;**12**:4098−121.
9. Aley KO, Reichling DB, Levine JD. Vincristine hyperalgesia in the rat: a model of painful vincristine neuropathy in humans. *Neuroscience* 1996;**73**:259−65.
10. Nozaki-Taguchi N, Chaplan SR, Higuera ES, Ajakwe RC, Yaksh TL. Vincristine-induced allodynia in the rat. *Pain* 2001;**93**:69−76.
11. Cavaletti G, Marmiroli P. Chemotherapy-induced peripheral neurotoxicity. *Nat Rev Neurol* 2010;**6**:657−66.
12. Weng HR, Cordella JV, Dougherty PM. Changes in sensory processing in the spinal dorsal horn accompany vincristine-induced hyperalgesia and allodynia. *Pain* 2003;**103**:131−8.
13. Cavaletti G, Marmiroli P. Chemotherapy-induced peripheral neurotoxicity. *Curr Opin Neurol* 2015;**28**:500−7.
14. Campbell JN, Meyer RA. Mechanisms of neuropathic pain. *Neuron* 2006;**52**:77−92.
15. Costigan M, Scholz J, Woolf CJ. Neuropathic pain: a maladaptive response of the nervous system to damage. *Annu Rev Neurosci* 2009;**32**:1−32.
16. Coste B, Mathur J, Schmidt M, Earley TJ, Ranade S, Petrus MJ, et al. Piezo1 and Piezo2 are essential components of distinct mechanically activated cation channels. *Science* 2010;**330**:55−60.
17. Wu J, Lewis AH, Grandl J. Touch, Tension, and transduction—the function and regulation of Piezo ion channels. *Trends Biochem Sci* 2017;**42**:57−71.
18. Murthy SE, Dubin AE, Patapoutian A. Piezos thrive under pressure: mechanically activated ion channels in health and disease. *Nat Rev Mol Cell Biol* 2017;**18**:771−83.
19. Drew LJ, Wood JN, Cesare P. Distinct mechanosensitive properties of capsaicin-sensitive and -insensitive sensory neurons. *J Neurosci* 2002;**22**:RC228.
20. Hu J, Lewin GR. Mechanosensitive currents in the neurites of cultured mouse sensory neurones. *J Physiol* 2006;**577**:815−28.

21. Delmas P, Hao J, Rodat-Despoix L. Molecular mechanisms of mechanotransduction in mammalian sensory neurons. *Nat Rev Neurosci* 2011;**12**:139−53.
22. Ranade SS, Woo SH, Dubin AE, Moshourab RA, Wetzel C, Petrus M, et al. Piezo2 is the major transducer of mechanical forces for touch sensation in mice. *Nature* 2014;**516**:121−5.
23. Ikeda R, Cha M, Ling J, Jia Z, Coyle D, Gu JG. Merkel cells transduce and encode tactile stimuli to drive Aβ-afferent impulses. *Cell* 2014;**157**:664−75.
24. Woo SH, Ranade S, Weyer AD, Dubin AE, Baba Y, Qiu Z, et al. Piezo2 is required for Merkel-cell mechanotransduction. *Nature* 2014;**509**:622−6.
25. Zhang M, Wang Y, Geng J, Zhou S, Xiao B. Mechanically activated Piezo channels mediate touch and suppress acute mechanical pain response in mice. *Cell Rep* 2019;**26**: 1419−1431.e4.
26. Shin SM, Moehring F, Itson-Zoske B, Fan F, Stucky CL, Hogan QH, et al. Piezo2 mechanosensitive ion channel is located to sensory neurons and nonneuronal cells in rat peripheral sensory pathway: implications in pain. *Pain* 2021;**162**:2750−68.
27. Chesler AT, Szczot M, Bharucha-Goebel D, Čeko M, Donkervoort S, Laubacher C, et al. The role of PIEZO2 in human mechanosensation. *N Engl J Med* 2016;**375**:1355−64.
28. Szczot M, Liljencrantz J, Ghitani N, Barik A, Lam R, Thompson JH, et al. PIEZO2 mediates injury-induced tactile pain in mice and humans. *Sci Transl Med* 2018;**10**:eaat9892.
29. Murthy SE, Loud MC, Daou I, Marshall KL, Schwaller F, Kühnemund J, et al. The mechanosensitive ion channel Piezo2 mediates sensitivity to mechanical pain in mice. *Sci Transl Med* 2018;**10**:eaat9897.
30. Du X, Hao H, Yang Y, Huang S, Wang C, Gigout S, et al. Local GABAergic signaling within sensory ganglia controls peripheral nociceptive transmission. *J Clin Invest* 2017;**127**:1741−56.
31. Zhang D, Men H, Zhang L, Gao X, Wang J, Li L, et al. Inhibition of M/Kv7 currents contributes to chloroquine-induced itch in mice. *Front Mol Neurosci* 2020;**13**:105.
32. Jia Z, Ikeda R, Ling J, Viatchenko-Karpinski V, Gu JG. Regulation of Piezo2 mechanotransduction by static plasma membrane tension in primary afferent neurons. *J Biol Chem* 2016;**291**:9087−104.
33. Hochmuth RM. Micropipette aspiration of living cells. *J Biomech* 2000;**33**:15−22.
34. Saville DJ. Basic statistics and the inconsistency of multiple comparison procedures. *Can J Exp Psychol* 2003;**57**:167−75.
35. Jia Z, Ikeda R, Ling J, Gu JG. GTP-dependent run-up of Piezo2-type mechanically activated currents in rat dorsal root ganglion neurons. *Mol Brain* 2013;**6**:57.
36. Alcaino C, Knutson K, Gottlieb PA, Farrugia G, Beyder A. Mechanosensitive ion channel Piezo2 is inhibited by D-GsMTx4. *Channels* 2017;**11**:245−53.
37. Dina OA, McCarter GC, de Coupade C, Levine JD. Role of the sensory neuron cytoskeleton in second messenger signaling for inflammatory pain. *Neuron* 2003;**39**:613−24.
38. Samson F, Donoso JA, Heller-Bettinger I, Watson D, Himes RH. Nocodazole action on tubulin assembly, axonal ultrastructure and fast axoplasmic transport. *J Pharmacol Exp Therapeut* 1979;**208**:411−7.
39. Szczot M, Pogorzala LA, Solinski HJ, Young L, Yee P, Le Pichon CE, et al. Cell-type-specific splicing of Piezo2 regulates mechanotransduction. *Cell Rep* 2017;**21**:2760−71.
40. Prato V, Taberner FJ, Hockley JRF, Callejo G, Arcourt A, Tazir B, et al. Functional and molecular characterization of mechanosensitive "silent" nociceptors. *Cell Rep* 2017;**21**:3102−15.
41. Eijkelkamp N, Linley JE, Torres JM, Bee L, Dickenson AH, Gringhuis M, et al. A role for Piezo2 in EPAC1-dependent mechanical allodynia. *Nat Commun* 2013;**4**:1682.
42. Poole K, Herget R, Lapatsina L, Ngo HD, Lewin GR. Tuning Piezo ion channels to detect molecular-scale movements relevant for fine touch. *Nat Commun* 2014;**5**:3520.
43. Qi Y, Andolfi L, Frattini F, Mayer F, Lazzarino M, Hu J. Membrane stiffening by STOML3 facilitates mechanosensation in sensory neurons. *Nat Commun* 2015;**6**:8512.
44. Tanner KD, Levine JD, Topp KS. Microtubule disorientation and axonal swelling in unmyelinated sensory axons during vincristine-induced painful neuropathy in rat. *J Comp Neurol* 1998;**395**:481−92.
45. Topp KS, Tanner KD, Levine JD. Damage to the cytoskeleton of large diameter sensory neurons and myelinated axons in vincristine-induced painful peripheral neuropathy in the rat. *J Comp Neurol* 2000;**424**:563−76.
46. Huang M, Chalfie M. Gene interactions affecting mechanosensory transduction in *Caenorhabditis elegans*. *Nature* 1994;**367**:467−70.
47. Wetzel C, Hu J, Riethmacher D, Benckendorff A, Harder L, Eilers A, et al. A stomatin-domain protein essential for touch sensation in the mouse. *Nature* 2007;**445**:206−9.
48. Hu J, Chiang LY, Koch M, Lewin GR. Evidence for a protein tether involved in somatic touch. *EMBO J* 2010;**29**:855−67.
49. Kanda H, Gu JG. Membrane mechanics of primary afferent neurons in the dorsal root ganglia of rats. *Biophys J* 2017;**112**:1654−62.
50. Raucher D, Sheetz MP. Characteristics of a membrane reservoir buffering membrane tension. *Biophys J* 1999;**77**:1992−2002.
51. White JG, Burris SM, Tukey D, Smith II C, Clawson CC. Micropipette aspiration of human platelets: influence of microtubules and actin filaments on deformability. *Blood* 1984;**64**:210−4.
52. Raucher D, Sheetz MP. Membrane expansion increases endocytosis rate during mitosis. *J Cell Biol* 1999;**144**:497−506.
53. Chang W, Gu JG. Impairment of tactile responses and Piezo2 channel mechanotransduction in mice following chronic vincristine treatment. *Neurosci Lett* 2019;**705**:14−9.
54. Chang W, Gu JG. Role of microtubules in Piezo2 mechanotransduction of mouse Merkel cells. *J Neurophysiol* 2020;**124**:1824−31.